Perspectives in Plant Ecology, Evolution and Systematics 64 (2024) 125800

Contents lists available at ScienceDirect

Perspectives in Plant Ecology, Evolution and Systematics

journal homepage: www.elsevier.com/locate/ppees

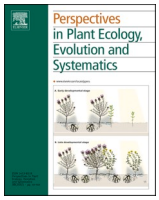

Phylogeography of the Euro-Siberian steppe plant *Astragalus austriacus*: Late Pleistocene climate fluctuations fuelled formation and expansion of two main lineages from a Pontic-Pannonian area of origin

Clemens Maylandt [a,1], Anna Seidl [b,1], Philipp Kirschner [a,c], Simon Pfanzelt [d,e], Gergely Király [f], Barbara Neuffer [g], Frank R. Blattner [d], Herbert Hurka [g], Nikolai Friesen [h], Alexander V. Poluyanov [i], Petr A. Kosachev [j], Corinna Schmiderer [b], Karl-Georg Bernhardt [b], Karin Tremetsberger [b,*]

[a] *Department of Botany, Universität Innsbruck, Sternwartestraße 15, Innsbruck 6020, Austria*
[b] *Institute of Botany, Department of Integrative Biology and Biodiversity Research, Gregor-Mendel-Straße 33, Vienna 1180, Austria*
[c] *Faculty of Agricultural, Environmental and Food Sciences, Free University of Bozen-Bolzano, Bolzano, Italy*
[d] *Experimental Taxonomy, Leibniz Institute of Plant Genetics and Crop Plant Research, Corrensstraße 3, Gatersleben 06466, Germany*
[e] *Botanical Garden Munich-Nymphenburg, Menzinger Straße 67, Munich 80638, Germany*
[f] *Faculty of Forestry, University of Sopron, Bajcsy-Zsilinszky utca 4, Sopron 9400, Hungary*
[g] *School of Biology/Chemistry, Osnabrück University, Barbarastraße 11, Osnabrück 49076, Germany*
[h] *Botanical Garden, Osnabrück University, Albrechtstraße 29, Osnabrück 49076, Germany*
[i] *Kursk State University, Radishcheva 33, Kursk 305000, Russia*
[j] *South-Siberian Botanical Garden, Altai State University, Lenina 61, Barnaul 656049, Russia*

ARTICLE INFO

Keywords:
Demography
Genotyping-by-sequencing
Molecular dating
Transylvanian Basin
Western Siberia

ABSTRACT

The Euro-Siberian steppes have experienced large-scale range fluctuations due to the climatic changes of the Pleistocene that may have also fuelled reshuffling of past steppe vegetation. These species-rich steppe grasslands were much more widespread during glacials and contracted during interglacials, a dynamic which should also be reflected by the evolutionary history of their biota. *Astragalus austriacus* is a widespread steppe species with European-western Siberian distribution and an ideal model to study the florogenesis of the Euro-Siberian steppes. Here, we inferred the phylogeography of *A. austriacus* based on genotyping-by-sequencing (GBS) data from populations sampled from the western edge of the Pannonian region across the Pontic region to the western Siberian region. Additionally, we applied molecular dating using single gene sequence data (*ycf*1, *mat*K and ITS). We outline an evolutionary scenario in which intraspecific diversification occurred in the eastern part of Europe during the later Pleistocene (0.48–0.24 Ma). From there, the species expanded both eastwards and westwards, likely during a cold period, which is reflected by two main lineages within *A. austriacus* that today occur in the Pannonian sensu lato and in the Pontic/south-western Siberian regions, respectively. Demographic modelling supported such a scenario and showed that population sizes were larger during the last cold stage and contracted postglacially. Within the Pannonian sensu lato region, strong substructure was detected, likely as a result of repeated disintegration of the continuous cold-stage steppes in Europe. Finally, our results are in line with evolutionary scenarios suggested for other steppe species such as *Adonis vernalis*.

1. Introduction

The Palaearctic steppe biome includes the European, Middle Asian, Mongolian (= Central Asian), Tibetan, and Mediterranean chorological-climatic subtypes (Wesche et al., 2016). Zonal grass and desert steppes occur in climates that are too dry to sustain the growth of forests and are

* Corresponding author.
E-mail addresses: maylandt.c@gmail.com (C. Maylandt), seidlonno@gmail.com (A. Seidl), philipp.kirschner@gmail.com (P. Kirschner), pfanzelt@snsb.de (S. Pfanzelt), karl-georg.bernhardt@boku.ac.at (K.-G. Bernhardt), karin.tremetsberger@boku.ac.at (K. Tremetsberger).
[1] These authors contributed equally to this work.

https://doi.org/10.1016/j.ppees.2024.125800
Received 26 December 2023; Received in revised form 24 March 2024; Accepted 31 May 2024
Available online 3 June 2024

regularly affected by frost. The ecological-physiognomic subtypes of steppe include forest-steppe, typical steppe, desert steppe, and alpine (mountain) steppe (Wesche et al., 2016). They are bordered by temperate or boreal forests in the north and semi-deserts in the south and are characterized by a high species richness with up to 98 plant species per 10 m^2 (Polyakova et al., 2016; Wilson et al., 2012). Our focus is on the Euro-Siberian steppes, which correspond to the European and Middle Asian chorological-climatic subtypes of Wesche et al. (2016) and comprise the Pontic-southern (actually south-western) Siberian floristic region of Meusel et al. (1965), which includes the forest-steppes of south-eastern Europe and (from north to south in a latitudinal zonation) the forest-steppes, long grass steppes and short grass steppes of eastern Europe and south-western Siberia (Middle Asia). Smaller patches of extrazonal grasslands in the west, which can nowadays be regarded as isolated islands surrounded by a sea of forest (Kirschner et al., 2022), resemble zonal steppes in several respects, i.e., in their species composition. In contrast to zonal steppes, these species-rich extrazonal steppes naturally occur under a continentally influenced climate wherever edaphic conditions do not allow the formation of a closed forest (Braun-Blanquet, 1961; Braun-Blanquet and de Bolós, 1957; Kajtoch et al., 2016; Kirschner et al., 2020; Magnes et al., 2021).

Our knowledge of the climate and landscape history of the Euro-Siberian steppe region has recently been supplemented by extensive and large-scale phylogeographical studies of plant and animal taxa (partly reviewed in Hurka et al., 2019). The extent of the Eurasian steppes was mainly driven by recurrent climatic changes during the Pleistocene, with steppes expanding during cold stages such as the last glacial (115–11.7 ka) and shrinking during warm stages such as the last interglacial (130–115 ka) (Binney et al., 2017). This had a large impact on steppe flora and fauna and has facilitated large-scale fluctuations of population sizes in synchrony with these climatic oscillations (Kirschner et al., 2022), and formation of allopatric lineages (Friesen et al., 2020; Kajtoch et al., 2016; Kirschner et al., 2020; Seidl et al., 2022; Willner et al., 2021; Záveská et al., 2019; Žerdoner Čalasan et al., 2021) and species due to range shifts and isolation in warm stage refugia (Baca et al., 2023; Kirschner et al., 2023; Vojtěchová et al., 2023). Regarding such range alterations, most available evidence points to a scenario in which steppe species were forced to retreat into refugia during Pleistocene warm stages. However, such refugial dynamics might not apply to all species and not in all parts of the Eurasian steppes, as the response of a species to a changing environment ultimately depends on species-specific ecological requirements, especially concerning temperature, precipitation and competition (Hurka et al., 2019; Stewart et al., 2010). The fact that steppe plant communities as we observe them in today's warm stage conditions probably did not exist in this composition in cold stages (Chytrý et al., 2019) renders modelling of refugial dynamics based on only climatic variables difficult, underlining the importance of phylogeographic studies based on genetic information, some of which already revealed different evolutionary histories of steppe biota. For example, *Krascheninnikovia ceratoides* (L.) Gueldenst. (Seidl et al., 2020, 2021) and *Astragalus onobrychis* L. (Záveská et al., 2019; Kirschner et al., 2020) originated in the early phases of the Pleistocene, one in western Central Asia or the Altai Region (*K. ceratoides*) the other in the Caucasus region (*A. onobrychis*), which allowed formation of various lineages in response to Pleistocene climatic oscillations. The eastern lineage of *Adonis vernalis* L., in contrast, evolved more recently, in the later phases of the Pleistocene, in south-eastern Europe (Seidl et al., 2022). The lack of a consistent pattern in these earlier studies prompted us to investigate another species.

Astragalus austriacus is a submeridional-continental species with a western European to south-western Siberian distribution. The range of *A. austriacus* includes isolated outposts in north-eastern Spain (montane scrubland on calcareous or loamy substrates at 600–1550 m a.s.l.) and the south-western Alps (dry valleys in the Cottian Alps at 1200–1400 m; Hegi et al., 1975; Podlech, 1999). It occurs in steppe-like habitats throughout its distribution range and was traditionally used to outline the Pontic-southern Siberian floristic region (Meusel et al., 1965). Apart from the zonal steppes, the species grows in extrazonal dry grasslands dominated by narrow-leaved tussock-forming grasses (*Festuca* Tourn. ex L., *Stipa* L.) and at the edges of thermophilous woods, usually on base-rich soil including loess (Hegi et al., 1975; Kaplan et al., 2016; see Fig. 1). Floristically, *A. austriacus* has been classified as a characteristic species of the south-eastern European forest-steppe zone (Erdős et al., 2018) and the Pannonian and western Pontic steppe grasslands (diagnostic for the order Festucetalia valesiacae; Willner et al., 2017). In competition with larger herbs and grasses, the species is disadvantaged and prefers pioneer (sometimes disturbed) habitats on open soil surfaces. In eastern Europe (Ukraine, European Russia, North Caucasus) and south-western Siberia, *A. austriacus* also grows in grass steppes with *Stipa* and *Festuca* species, on limestone in pine woods, and rarely in old fallows (Borisova et al., 1946, English translation 1986). In Middle Asia, at the southern edge of its range, in the transition from the southern Siberian to the Aralo-Caspian floristic province (Meusel et al., 1965), the species becomes rare and grows in humid shallow depressions or dry saline steppes. According to traditional taxonomy, the species belongs to the sect. *Craccina* Bunge (Bunge, 1868; Podlech and Zarre, 2013) while the phylogenetic placement of *A. austriacus* within *Astragalus* remains to be tested.

In this study, we aimed to disentangle the phylogeography and evolutionary history of *Astragalus austriacus* in its main distribution range in the Pannonian region, the Pontic region and south-western Siberia. Given that this species is a typical Euro-Siberian steppe element, this allows us to shed light on the florogenesis of the Euro-Siberian steppes and underlying evolutionary dynamics. Specifically, we asked: i) When and where did the recent populations of *A. austriacus* growing in the Euro-Siberian steppes originate, and what was the effect of Pleistocene climate fluctuations? ii) Are the spatial and temporal patterns found in *A. austriacus* similar to that of other typical Euro-Siberian steppe species? To answer these questions, we employed phylogenetic, clustering and demographic analyses based on genotyping-by-sequencing (GBS) data that was complemented by dated phylogenies derived from single-gene sequencing. The similarity in the distribution pattern of *A. austriacus* and *Adonis vernalis* (Seidl et al., 2022) led us to hypothesize that both species may have undergone a similar evolutionary history.

2. Material and methods

2.1. Sampling of plant material and extraction of DNA

Populations of *A. austriacus* from Austria in the west to Kazakhstan in the east were collected, with one to six individuals per population (total: 71 individuals, 18 populations, mean per population: 3.94; see Appendix A), covering a major part of the species' continuous distribution area but with sample gaps between the three major areas sampled (Fig. 1–3). Outposts from Spain and the south-western Alps were not included as they were out of the scope of this study. In our usage, "Pannonian s.lat." includes not only the central Pannonian Basin with its western transition areas to Moravia (Czech Republic) and the eastern Alps (here referred to as "Pannonian s.str.") but also the continental parts of the Transylvanian Basin (Fekete et al., 2016). In addition, we collected individuals from populations of four other *Astragalus* species to be used as outgroups (Appendix B). We placed the leaf material of the individuals in the field in silica gel to preserve the DNA and usually collected one voucher per site (deposited at WHB; Appendices A, B). We extracted DNA from approximately 20 mg of silica gel-dried leaf material with the innuPREP Plant DNA Kit using the SLS lysis solution containing CTAB (Analytic Jena, Jena, Germany), the DNeasy Plant Mini Kit (Qiagen, Hilden, Germany) or the NucleoSpin Plant II kit (Macherey-Nagel, Düren, Germany) according to the manufacturers' instructions and determined the DNA concentration of the extracts in a DS-11 FX Fluorometer (DeNovix, Wilmington, Delaware, USA) using the DeNovix dsDNA Broad Range

Fig. 1. Current distribution and habitats of *Astragalus austriacus*. Map: The orange area indicates the distribution after Meusel et al. (1965), brown squares indicate the distribution proposed by Jäger (1971) in Spain. Points reflect the locations according to GBIF records (only accessions based on herbarium specimens were used). Red crosses show areas in Italy for which occurrences of *A. austriacus* were suggested in the past (Meusel et al., 1965) but actually never have been confirmed (Pignatti, 2017; T. Wilhalm, personal communication, June 21, 2023). Blue, green and pink circles indicate the areas sampled in this study (see Fig. 2 for details). Left: Austria, Blauer Berg SE of Oberschoderlee. *Astragalus austriacus* is growing here on the field path on top of the steep loess hill, where it is exposed to disturbance by agricultural vehicles. The locality is known as a Holocene refugium for the dry steppe and semi-desert plant *Krascheninnikovia ceratoides*. Another characteristic plant of open loess steppes growing here is *Taraxacum serotinum*. Right: Hungary, glacial terrace SE of Nagyszentjános. Meadow steppe with, among many others, *Stipa pennata* (s.str.), *A. austriacus*, *A. exscapus*, *A. onobrychis* and *Adonis vernalis*.

Assay (DeNovix).

2.2. Genotyping-by-sequencing (GBS)

For the preparation of the GBS library, we digested 200 ng of genomic DNA from each individual with the restriction enzymes *Pst*I-HF and *Msp*I (New England Biolabs, Ipswich, Massachusetts, USA) following published protocols (Wendler et al., 2014). Two individuals were used twice to produce the library to assess the reproducibility of the method. The multiplexed samples were sequenced on separate lanes in two consecutive runs on a HiSeq 2500 system (Illumina, San Diego, California, USA; single-end reads, sequence lengths approximately 100 bp). Processing of GBS raw data was done with ipyrad (Eaton and Overcast, 2020), first with the samples of the in- and outgroup together (Appendices A, B), second with the samples of the ingroup only (*A. austriacus*; Appendix A). As *A. austriacus* is diploid ($2n = 16$ chromosomes; Bartha et al., 2013; Dvořák et al., 1977; Podlech and Zarre, 2013), we allowed up to two alleles per individual and site. With ipyrad, we removed the restriction site overhangs "TGCAG" and "CGG" and applied the strict adapter filtering option to also remove the Illumina adapters. Setting the Phred quality score to 33, we filtered reads that had more than five poor quality base calls. For de novo assembly and single nucleotide polymorphism (SNP) calling, we allowed a maximum of eight indels, 20 % SNPs and 50 % of samples sharing heterozygous sites for a locus, 5 % uncalled bases and 5 % heterozygous sites in the consensus sequence and used a threshold of 85 % sequence similarity of reads to be considered reads at the same locus. We specified that at least 10 % of all individuals should have data at each locus and that only loci with a depth of six to 10,000 and a minimum length of 35 bp should be retained. Further, we had the ploidy level of the individuals estimated as described in Seidl et al. (2021) using the two software programs nQuire (applying the denoising option; Weiß et al., 2018) and ploidyNGS (applying the guess ploidy option; Corrêa dos Santos et al., 2017).

2.3. Downstream analysis of GBS data

Phylogenetic analyses were performed on the dataset including outgroups with 151,831 distinct alignment patterns in RAxML v. 8.2.12 under the GTR+G model, and 1000 rapid bootstrap inferences were executed (Stamatakis, 2014; Stamatakis et al., 2008).

To determine the number of ancestral populations and calculate the (private) allelic richness, we first removed the replicate of one

individual from population P14 (Rostov) from the GBS dataset of *Astragalus austriacus* as well as five individuals that appeared to be clonal offshoots, namely one from population P3 (Fertőrákos), one from population P8 (Pănet), and three from population P15 (Proletarka; Fig. 2). We determined the population genetic structure using the LEA package (Frichot and François, 2015) in R v. 3.5.0, using the ingroup dataset of unlinked SNPs in the Variant Call Format (VCF). We tested the number *K* of ancestral populations with 100 replicates each and selected the correct number based on the minimal cross-entropy. Ultimately, we plotted the membership to each ancestral population (genetic group) of each population (as the mean across its individuals).

To calculate the (private) allelic richness, we converted the dataset to the Genepop format required by HP-Rare (Kalinowski, 2005) by coding alleles, not SNPs. Only loci called in at least one individual in each population were used (5038 such loci). We calculated the allelic richness (Ar) and private allelic richness (pAr) per biogeographic region and per population. The rarefaction sample sizes were two populations from each region and two nucleobases from each population.

Past changes in effective population size (N_e) were modelled on the basis of the folded site frequency spectrum (SFS) using the software Stairway Plot 2 (Liu and Fu, 2020). Modelling was done separately for each group as resolved by LEA, i.e., the Pannonian group (22 individuals from populations P1–P5), the Transylvanian group (13 individuals from populations P6–P8) and the Pontic group (25 individuals from populations P9–P13 and P15), omitting the probable clonal offshoots in P3, P8 and P15 as well as the population P14. As the eastern Pontic (P16) and south-western Siberian populations (P17 and P18) formed a separate group (Fig. 2), they were excluded to avoid distorting demographic signal by excessive genetic substructure. Group wise SFS were inferred based on a single SNP per fragment and the number of alleles was down projected to maximise the number of segregating sites. Calculations and down projections were done via the python script easySFS.py (https://github.com/isaacovercast/easySFS) that utilises the package *dadi* (Gutenkunst et al., 2009). Underlying GBS data was exported from ipyrad as VCF file and pre-processed in VCFtools (Danecek et al., 2011), and prior to each modelling run, loci missing from more than 20 % (–max-missing 0.8) of all individuals, and loci with mean read depths below five and above 100 (–min-meanDP 5 and –max-meanDP 100) were removed. For inferring demographic parameters, a mutation rate of 7×10^{-9} substitutions per site per generation (Ossowski et al., 2010) and a generation time of ten years were used. The latter estimate roughly corresponds with observations from ecologically similar *Astragalus* species from dry grasslands (Compagnoni et al., 2021).

2.4. Sanger sequencing and alignment

Amplifications of the plastid region *ycf*1 were performed in 20 μL reactions comprising 8 μL REDTaq PCR Reaction Mix (Sigma-Aldrich), 0.9 μL BSA (1 mg/ml; Promega), 0.55 μL (10 μM) of both primers (AO_f and AO_r; Záveská et al., 2019) and 1 μL of 1:10 diluted DNA extract. Cycling parameters for 35 cycles were 30 s at 98 °C, 10 s at 98°C, 30 s at 58 °C and 30 s at 72 °C followed by a final extension step at 72 °C for 10 min. The amplification of the ITS region of two samples of *Astragalus onobrychis* population 276 of Záveská et al. (2019) was carried out in 20 μL reactions using the same reagents as for *ycf*1 but the ITS primer pair 17SE and 26SE (Sun et al., 1994). To enhance the specificity of the primer pair, we used a touchdown PCR program of 35 cycles with 30 s at 94 °C, starting annealing temperature of 56 °C, which was decreased by 0.4 °C each cycle until 48° C from where on it stayed constant, 1 min at 72 °C. The final extension step was done with 72 °C for 10 min. After checking the amplicons on 1 % TBE agarose gels, they were purified enzymatically using Exonuclease I and Shrimp Alkaline Phosphatase (SAP; Fermentas) following the manufacturer's instructions. Sequencing was carried out at Eurofins Genomics using the same primers as for amplification.

Three primer combinations were used for amplification of *mat*K: trnK685F and matK832R; matK4La and matK1932Ra; and matK1100L and trnK2R* (Wojciechowski et al., 2004). For 15 μL PCR reactions, 1 μL DNA extract (diluted 1:20), 1× Red HS Taq Master Mix (Biozym, Vienna, Austria) and 400 nM of each primer (Microsynth, Vienna, Austria) were used. The initial denaturation step was at 95 °C for 2 min, followed by 40 cycles at 95/60/72 °C for 15/15/60 s and a final extension step at 72 °C for 7 min. For ITS of the remaining samples, the same PCR mix, but with the primers 17SE and 26SE (Sun et al., 1994), and program were used except for 58 °C annealing temperature. PCR products were checked on agarose gels and the remaining volume (13 μL per sample) was cleaned up with Exonuclease I (5.2 U) and FastAP Thermosensitive Alkaline Phosphatase (1 U) (Thermo Fisher Scientific, Waltham, Massachusetts, USA) at 37 °C for 15 min and 85 °C for 15 min. Sanger sequencing of *mat*K was performed in one direction only with primers matK832R, matK4La or matK1100L and of ITS in both directions with primers 17SE und ITS4 (White et al., 1990).

For *Astragalus austriacus*, two individuals each per population P14 to P16 were sequenced. From the 14 populations (P1–P3, P5–P13, P17, P18) one individual per population was investigated (Appendix A). To infer interspecific relationships in a broader context and for the molecular dating analyses, individuals of four closely related *Astragalus* species (*A. danicus* Retz., *A. onobrychis*, *A. sulcatus* L. and *A. tibetanus* Benth. ex Bunge; Appendix B) were also newly sequenced. Further, the generated sequences were complemented by six accessions from GenBank (*A. aduncus* Willd., *A. alpinus* L., *A. argyroides* Beck, *A. laxmannii* Jacq., *A. scaberrimus* Bunge and *A. viridis* Bunge; Appendix C) for each of the three examined genetic regions (ITS, *mat*K and *ycf*1). Sequences were aligned using MAFFT (http://mafft.cbrc.jp/alignment/server/). Subsequently the alignment was further improved manually in BioEdit v. 7.0.0 (Hall, 1999) and AliView (Larsson, 2014). The chromatograms of the ITS sequences were checked for double peaks with the software FinchTV v1.4.0 (Geospiza).

2.5. Dated phylogeny and haplotype network based on Sanger sequences

To reconstruct the phylogenetic relationships and to estimate divergence times within the Hypoglottis clade (Azani et al., 2017, 2019; Su et al., 2021), two separate datasets (1. nuclear: ITS; 2. cpDNA: *mat*K + *ycf*1) were analysed using the software BEAST v. 2.6.6 (Bouckaert et al., 2019). First, a matrix consisting of the chloroplast markers *mat*K and *ycf*1 of 19 sequences from eleven species was used. The trees of the two partitions were linked in BEAUti whereas all other properties related to the partitions were estimated independently. The ITS alignment consisted of 15 sequences from eleven species. Model testing was done with ModelFinder (Kalyaanamoorthy et al., 2017). After checking the BIC value, K80 + G4, F81 and TPM3uf + G4 were chosen for ITS, *mat*K and *ycf*1, respectively. To date, no reliable fossils are known that can be unambiguously assigned to *Astragalus* or closely related members in the (chloroplast) Inverted Repeat-Lacking Clade of legumes (Lavin et al., 2005; Wojciechowski, 2005). For this reason, the datasets were secondarily calibrated with the inferred ages from Su et al. (2021). The two chronograms in this study were calibrated at three nodes of clades determined to be monophyletic with normal priors: (1) the crown node of the Hypoglottis clade (mean = 4.76 Ma, 95 %HPD = 3.59–6.12 Ma), (2) the split between *A. onobrychis* and *A. tibetanus* (mean = 4.04 Ma, 95 %HPD = 3.0–5.1 Ma), and (3) the crown node of the group comprising *A. laxmannii*, *A. tibetanus* and (presumably) *A. austriacus* (mean 2.61 Ma, 95 %HPD = 2.0–3.2 Ma). The BEAST analyses were conducted using an uncorrelated lognormal relaxed clock model (Drummond et al., 2006) alongside the Calibrated Yule Model. All other priors in this panel were left as default. For each of the two datasets mentioned above, two independent analyses were run for 100 million generations sampling every 10,000 generations, which resulted in 2 × 10,000 trees. Log files were sampled every 1000 generations and analysed using Tracer v. 1.7 (Rambaut et al., 2018) to assess convergence and ensure that the effective sample size (ESS) for all parameters was

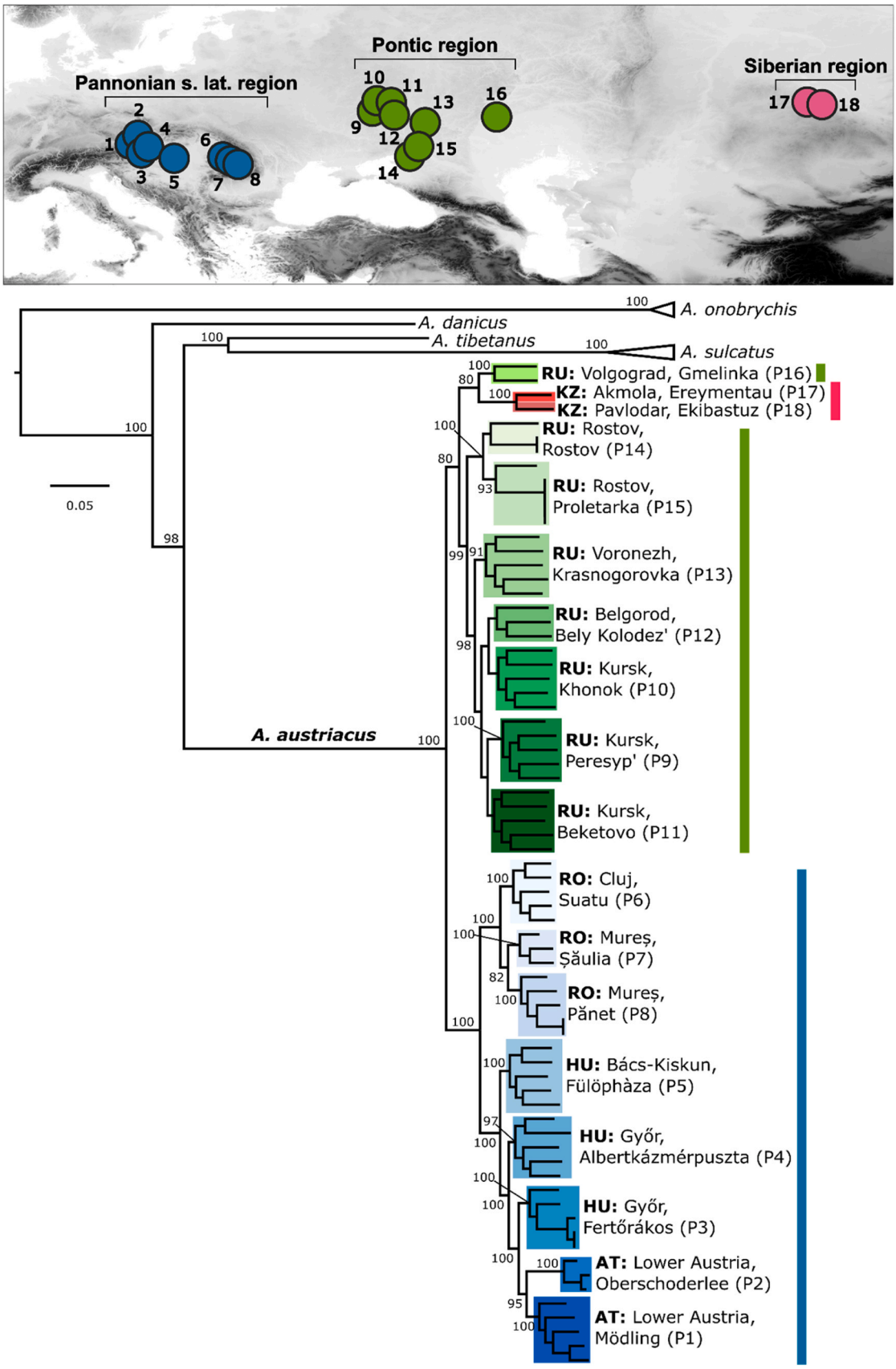

Fig. 2. Midpoint-rooted RAxML tree of *Astragalus austriacus* individuals genotyped with GBS. Outgroup species are collapsed. The colours refer to biogeographic regions. Bootstrap values greater than or equal to 80 % are shown for nodes at the population level or higher. Two-letter country abbreviations: AT – Austria, HU – Hungary, KZ – Kazakhstan, RO – Romania, RU – Russia.

>200. The tree files of the two independent runs were combined using LogCombiner v. 1.7.5 (Drummond and Rambaut, 2007). Subsequently, a maximum clade credibility (MCC) tree excluding the initial 10 % of trees as burn-in and showing median heights was constructed using TreeAnnotator v. 1.7.5 (Drummond and Rambaut, 2007). Finally, the trees were summarised using FigTree ver. 1.4 (http://tree.bio.ed.ac.uk/software/figtree/).

For the haplotype network, a concatenated alignment of *mat*K and *ycf*1, which consisted of 20 accessions from 17 populations of *Astragalus austriacus* and one individual of *A. danicus*, was used. The haplotype network was constructed using statistical parsimony as implemented in TCS 1.21 (Clement et al., 2000) with the software PopART (Leigh and Bryant, 2015). The analysis was run with the default parsimony connection limit of 95 % and indels were treated as missing data. The maps were produced with QGIS (http://www.qgis.org) and the basemap "GTOPO30" (https://www.usgs.gov/centers/eros/science/usgs-eros-archive-digital-elevation-global-30-arc-second-elevation-gtopo30).

3. Results

3.1. GBS data

The GBS raw data are available at the European Nucleotide Archive (accessions ERS10741157 to ERS10741268 under the study accession number PRJEB51106; Appendices A, B). The ipyrad alignment of *Astragalus austriacus* including outgroups in VCF format had 20,605 informative loci comprising 164,217 SNPs, of which 20,605 were unlinked SNPs. The samples had an average of 8858 SNPs (with a range of 5022 to 10,129 SNPs per sample). The alignment of *A. austriacus* without outgroups had 21,543 loci comprising 159,101 SNPs (21,543 unlinked). The samples of the ingroup had an average of 9601 SNPs (with a range of 5546 to 10,689 SNPs per sample). As can be seen from the RAxML tree (Fig. 2, Fig. S1), the replicates of an *A. austriacus* sample from P14 (Rostov) and of an *A. sulcatus* sample from Kalinovka (Kostanay Region, Kazakhstan) cannot be distinguished from the corresponding individual. Some other samples were also very similar (in the case of *A. austriacus*, four samples from P15 and two samples each from P3 and P8, and in the case of *A. sulcatus*, two samples from Krasnoarmeyskoe, Samara Oblast, Russia). The sampled individuals of *A. austriacus* were generally classified as diploid based on the GBS data by nQuire and ploidyNGS (eight out of 68 individuals = 11.7 % showed discrepancies between the two programs).

3.2. Clustering of A. austriacus populations and relationships based on GBS data

The most likely number of ancestral populations (K) in the LEA analysis based on minimal cross-entropy was $K = 3$, with $K = 3$ performing marginally better than $K = 2$. The LEA barplot (Fig. 3 A) shows the membership of individuals to the three genetic groups or ancestral populations (K). The first split ($K = 2$) separated the Pannonian sensu lato (s.lat.; Fekete et al., 2016) populations (P1–P8) from the Pontic/south-western Siberian populations (P9–P18; red). The second split ($K = 3$) occurred within the Pannonian s.lat. group and separated the western, i.e., Pannonian sensu stricto (s.str.) populations (P1–P5; blue) from the eastern, i.e., Transylvanian populations (P6–P8; yellow).

The basal node in the RAxML tree (Fig. 2) of *A. austriacus* separated the Pannonian s.lat. from the Pontic/south-western Siberian populations. The Pannonian s.lat. populations were divided into the Transylvanian populations (P6–P8) and the Pannonian s.str. populations (P1–P5). Within the Pannonian s.str. group, a successive branching of populations could be observed from east to west, namely from Bács-Kiskun County (Hungary; P5) through Győr-Moson-Sopron County (Hungary; P4 to P3) to the transition areas to the eastern Alps and Moravia (Lower Austria; P1 and P2). Within the Pontic/south-western Siberian group, the more westerly populations (P9–P15; Kursk, Belgorod, Voronezh and Rostov Oblasts in Russia) were separated from the more easterly populations (P16–P18; Volgograd Oblast in Russia and

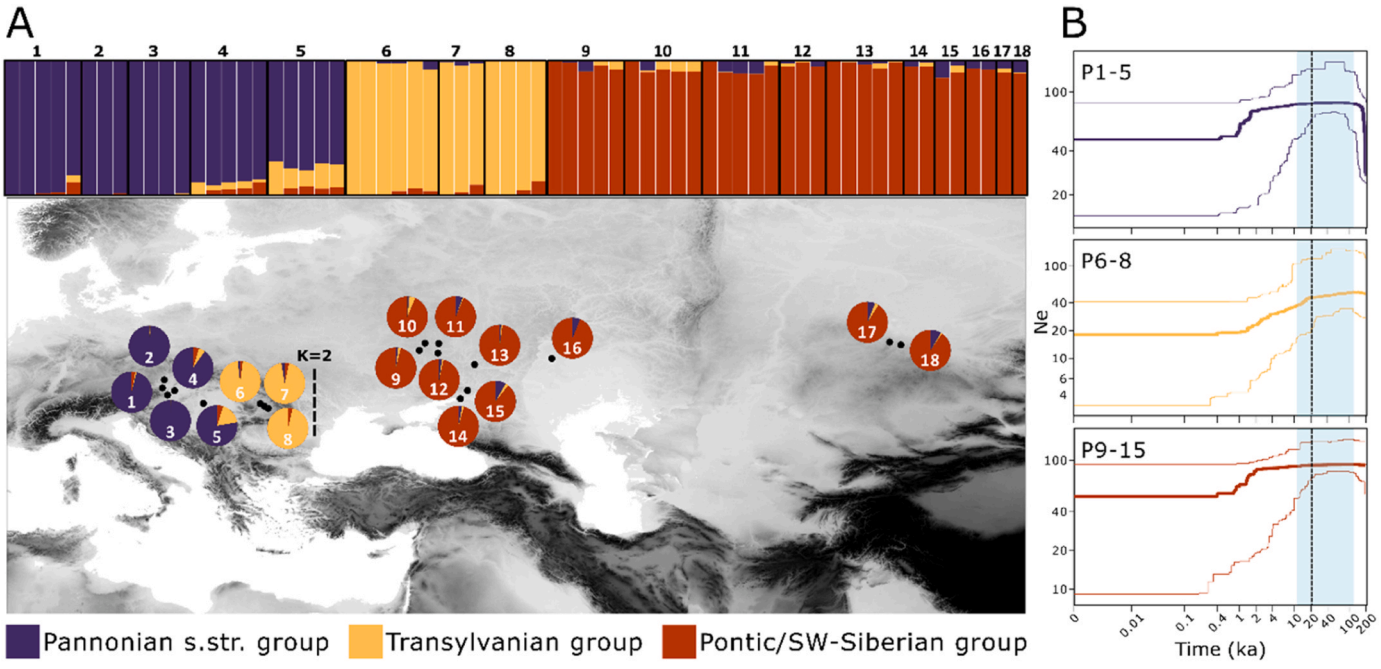

Fig. 3. (A) Distribution of shared genetic variation within *Astragalus austriacus* inferred by LEA (Frichot and François, 2015) on the basis of GBS data. Proportions are given for each individual (barplots) and on the level of populations (map) assuming K = 3. The dashed vertical line depicted in the map shows the split between Pannonian s.lat. and Pontic/Siberian populations for K = 2. (B) Demographic histories are shown as line plots that were inferred via Stairway Plot 2 (Liu and Fu, 2020). The lines represent the median estimates of effective population size N_e (bold line) and corresponding 95 % confidence intervals (thin lines) over time; axis scales are logarithmic, shaded blue areas indicate the last glacial period (11.7–115 ka), and the dashed line indicates the last glacial maximum (20 ka). SW stands for south-western.

Akmola and Pavlodar Regions in Kazakhstan).

3.3. Demographic history

Demographic analyses suggested a decline of N_e from the end of the last glacial period (LGP), intensifying towards the Holocene in all investigated groups (Fig. 3B). During large parts of the LGP N_e was stable, and increased at the end of the last interglacial and the onset of the LGP. Both the absolute values of N_e and the amplitude of N_e variation were comparable between the Pannonian s.str. and Pontic groups, while the Transylvanian group showed an earlier onset of the decline.

3.4. Geographic variation in allelic and private allelic richness based on GBS data

The values of Ar and pAr (Fig. S2) calculated directly for the biogeographic regions (by randomly selecting two populations per region; average ± standard error over 5038 GBS loci) correlate with the population values of Ar and pAr averaged for the regions (Table 1). Directly calculated Ar for the Pannonian s.lat. region is 1.89 ± 0.01, for the Pontic region 2.01 ± 0.01, and for the south-western Siberian region 1.80 ± 0.01. Directly calculated pAr for the Pannonian s.lat. region is 0.78 ± 0.01, for the Pontic region 0.79 ± 0.01, and for the south-western Siberian region 0.70 ± 0.01.

Table 1
Allelic richness (Ar) and private allelic richness (pAr; average ± standard error over 5038 GBS loci) of populations of *Astragalus austriacus* analysed in this study. Mean values over populations for biogeographic regions are also shown along with their standard deviations.

Population	Ar	pAr
Pannonian s.lat. region		
1. Austria, Lower Austria, Föhrenberge W of Mödling	1.36 ± 0.00	0.37 ± 0.01
2. Austria, Lower Austria, Blauer Berg SE of Oberschoderlee	1.27 ± 0.00	0.31 ± 0.01
3. Hungary, Győr-Moson-Sopron County, Fertőrákos	1.33 ± 0.00	0.34 ± 0.01
4. Hungary, Győr-Moson-Sopron County, Albertkázmérpuszta	1.38 ± 0.00	0.34 ± 0.01
5. Hungary, Bács-Kiskun County, Fülöpháza	1.39 ± 0.00	0.37 ± 0.01
6. Romania, Cluj County, NNW of Suatu	1.36 ± 0.00	0.34 ± 0.01
7. Romania, Mureș County, NNE of Șăulia	1.36 ± 0.00	0.34 ± 0.01
8. Romania, Mureș County, W of Târgu Mureș, SSE of Pănet	1.33 ± 0.00	0.31 ± 0.01
Mean ± standard deviation	**1.35 ± 0.04**	**0.34 ± 0.02**
Pontic region		
9. Russia, Kursk Oblast, Peresyp'	1.41 ± 0.00	0.36 ± 0.01
10. Russia, Kursk Oblast, N of Khonok	1.42 ± 0.00	0.38 ± 0.01
11. Russia, Kursk Oblast, Beketovo	1.43 ± 0.00	0.38 ± 0.01
12. Russia, Belgorod Oblast, Bely Kolodez' E of Novy Oskol	1.41 ± 0.00	0.36 ± 0.01
13. Russia, Voronezh Oblast, Krasnogorovka	1.43 ± 0.00	0.37 ± 0.01
14. Russia, Rostov Oblast, Rostov, Botanical Garden steppe reserve	1.34 ± 0.00	0.34 ± 0.01
15. Russia, Rostov Oblast, W of Proletarka	1.31 ± 0.00	0.37 ± 0.01
16. Russia, Volgograd Oblast, between Khar'kovka and Gmelinka	1.39 ± 0.01	0.38 ± 0.01
Mean ± standard deviation	**1.39 ± 0.04**	**0.37 ± 0.01**
South-western Siberian region (= Western Siberian Lowland)		
17. Kazakhstan, Akmola Region, between Ekibastuz and Ereymentau	1.28 ± 0.01	0.30 ± 0.01
18. Kazakhstan, Pavlodar Region, 75 km SW of Ekibastuz	1.27 ± 0.01	0.32 ± 0.01
Mean ± standard deviation	**1.28 ± 0.01**	**0.31 ± 0.01**

3.5. Spatial intraspecific patterns of plastid and ITS data

Based on the concatenated alignment of the plastid markers *mat*K and *ycf*1, we identified six haplotypes separated by a maximum of two mutational steps (Fig. 4). The basalmost H1 was found on the westernmost (Pannonian s.str. region) and easternmost (south-western Siberian region) limits of the sampled distribution of the species. The most frequent H2 was common throughout the Pannonian s.lat. and Pontic regions but did not occur in south-western Siberia. Four additional haplotypes (H3–H6) that each differed from H2 by one substitution were found in the Pontic area, which was the region harbouring most haplotypes (Pannonian s.lat. region: 2, Pontic region: 4, south-western Siberian region: 1). In the ITS data, three ribotypes were discovered. A common, widely distributed ribotype was shared by populations from the Pannonian s.lat. region and the Pontic region. In the westernmost limit of the sampled area (Pannonian s.str. region), a second ribotype was detected in a single population while the third ribotype characterized the two easternmost sampled populations from south-western Siberia.

3.6. Phylogenetic position of A. austriacus and age estimation

A time-tree of members of the Hypoglottis clade (Fig. 5) was calculated on the basis of two plastid markers *mat*K (1741 bp, 38 variable sites, 12 parsimony informative sites and one indel of eleven bp in *A. alpinus*) and *ycf*1 (908 bp, 134 variable sites, 74 parsimony informative sites, nine indels of various lengths from 3 to 30 bp). Derived substitution rates were 0.0008 substitutions/site/Million years (= s/s/Ma) for *mat*K and 0.009 s/s/Ma for *ycf*1. The backbone of the tree was maximally supported (PP = 1) with the ancestor of two main groups segregating from *A. alpinus* 4.91 Ma (95 %HPD = 3.98–5.88 Ma). The "*A. onobrychis* group" branched off 4.12 Ma (95 %HPD = 3.28–4.92 Ma) and started to differentiate in the Mid-Pleistocene 1.06 Ma (95 %HPD = 0.39–1.92 Ma). The other group comprising *A. argyroides*, *A. austriacus*, *A. danicus*, *A. laxmannii*, *A. scaberrimus*, *A. sulcatus*, *A. tibetanus* and *A. viridis* began to diversify 2.40 Ma (95 %HPD = 1.85–2.99 Ma), which coincides with the early Pleistocene. The *A. austriacus* lineages investigated here evolved 0.48 Ma (95 %HPD = 0.13–1.09 Ma) in the Mid-Pleistocene after the Mid-Pleistocene Transition (MPT). It is noteworthy that for the marker *ycf*1 alone a younger crown age of 0.28 Ma (95 %HPD = 0.04–0.74 Ma) was calculated for *A. austriacus* (data not shown), which was highly similar to the inferred crown age in the ITS time-tree (Fig. 6). In contrast to the nuclear data (GBS, ITS; Figs. 2, 6), *A. sulcatus* was polyphyletic in the plastid time-tree. One haplotype was found in two individuals of the same population from the Pontic region (Samara Oblast). This haplotype was associated with *A. tibetanus* and *A. danicus*, as is the case with ITS. Interestingly, the other haplotype of *A. sulcatus*, which was detected in all populations of the western Siberian region east of the Ural Mountains, is strikingly disparate and clustered in a distantly related group alongside with *A. viridis* and *A. argyroides*, both are members of the section *Dissitiflori* DC. (see Fig. 5).

A second time-tree of the Hypoglottis clade (Fig. 6) was inferred based on the ITS alignment (603 bp, 49 variable sites, 17 parsimony informative sites, one indel of 7 bp and a deletion of one base in *A. alpinus*). A substitution rate of 0.0034 s/s/Ma was calculated. Although slightly incongruent with the tree inferred from plastid markers, the topology of the ITS time-tree as well resolved the "*A. onobrychis* group" (PP = 0.91) as a sister to the remainder of the taxa (PP = 1) after the initial divergence of *A. alpinus*. Separation from *A. alpinus* occurred 5.12 Ma (95 %HPD = 4.13–6.17 Ma). The "*A. onobrychis* group" and its sister group shared a common ancestor 3.35 Ma (95 %HPD = 2.58–4.26 Ma). Subsequently, the "*A. onobrychis*

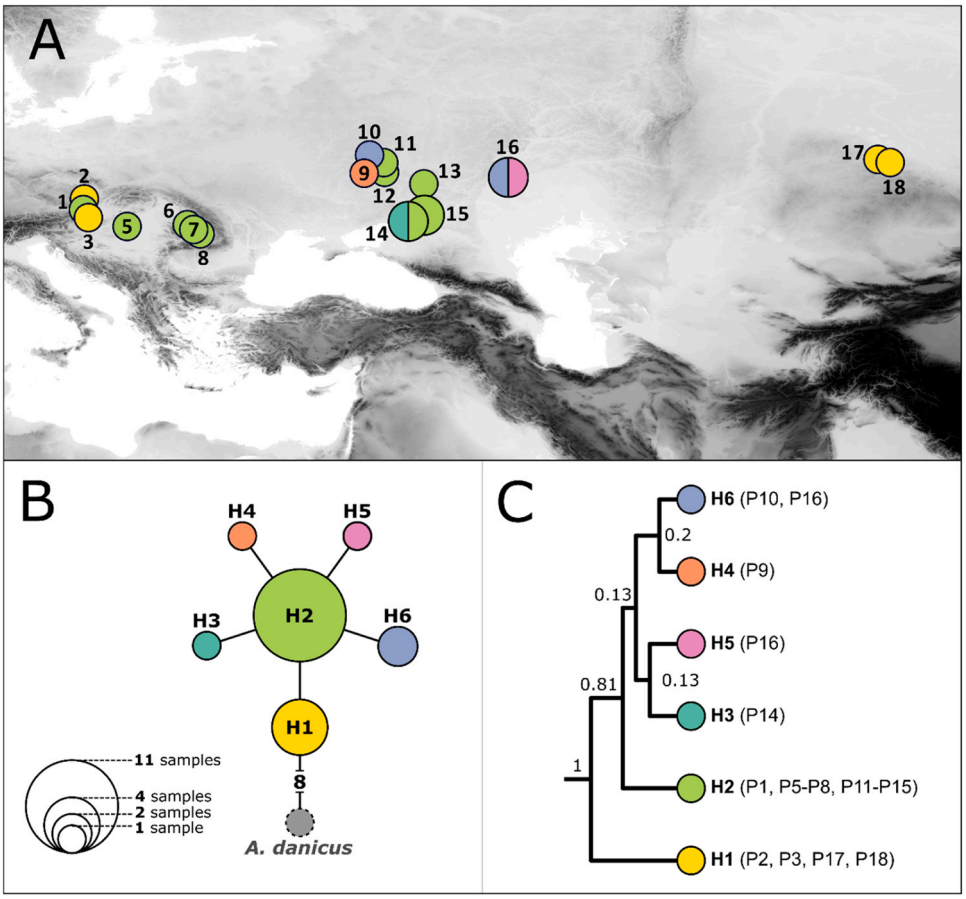

Fig. 4. Plastid haplotype distribution of *A. austriacus* based on *ycf*1 and *mat*K sequences. (A) shows the spatial distribution of haplotypes across the sampled area. (B) illustrates the haplotype network, rooted with *A. danicus*. (C) represents the intraspecific relationships inferred with the BEAST analysis.

group" diversified 2.29 Ma (95 %HPD = 1.13–3.41 Ma), and the remaining taxa started to differentiate 2.65 Ma (95 %HPD = 2.12–3.18 Ma) at the beginning of the Pleistocene. Similar to the results based on the plastid markers, the crown age of *A. austriacus* was dated to 0.24 Ma (95 %HPD = 0.01–0.66 Ma) in the Mid-Pleistocene after the MPT.

4. Discussion

4.1. *Astragalus austriacus* – a recently evolved species of the highly diverse Hypoglottis clade

Astragalus austriacus was classified as diploid based on the GBS data, which is consistent with previous reports (Bartha et al., 2013; Dvořák et al., 1977; Podlech and Zarre, 2013). It was related to *A. tibetanus* (sect. *Hypoglottidei* DC.) and *A. sulcatus* (sect. *Craccina*) in the GBS phylogeny (Fig. 2) and in addition showed a sister relationship to members of the section *Dissitiflori* in the single-gene phylogenies (Figs. 5, 6). Thus, the species belongs to the most derived, highly diverse and species-rich Hypoglottis clade, which has been proposed by Azani et al. (2017, 2019) based on genetic data.

We found that the group including *A. austriacus* and close allies split at the onset of the Pleistocene (ITS: 2.65 Ma, cpDNA: 2.40 Ma; Figs. 5, 6). The early Pleistocene was a period of extensive speciation and diversification within the genus *Astragalus*, with larger diversification rates in later phases of the Pleistocene (Amini et al., 2019; Azani et al., 2019; Bagheri et al., 2017, 2023; Hardion et al., 2016; Su et al., 2021; Záveská et al., 2019). In line with these previous findings, diversification between the *A. austriacus* lineages investigated here occurred after the MPT (ITS: 0.24 Ma; *ycf*1 + *mat*K: 0.48 Ma; *ycf*1: 0.28 Ma) when cold and dry glacial stages became more intense and significantly longer (Hays et al., 1976; Herbert, 2023) while the stem age of these lineages is somewhat older based on our sampling (ITS: 1.03 Ma; *ycf*1 + *mat*K: 1.68 Ma).

Incongruences between the nuclear (GBS, ITS) and plastid data observed in *A. sulcatus* (Figs. 5, 6, Fig. S1) might indicate horizontal gene flow in the genealogy of its western Siberian populations. Only the Pontic population harboured the plastid haplotype closely related to *A. tibetanus* and *A. danicus*, which is expected from the nuclear data and a published *ycf*1 sequence from a Transylvanian *A. sulcatus* individual (Bartha et al., 2012). The chloroplast found in the western Siberian populations, however, clusters with representatives of sect. *Dissitiflori* (Fig. 5). This finding is in line with previous works that already suggested the occurrence of hybridization and reticulate speciation in the genus *Astragalus* (Kazemi et al., 2009; Bartha et al., 2013; Záveská et al., 2019).

4.2. *Astragalus austriacus* lineages of the main distribution area evolved in the eastern part of Europe in the later Pleistocene and expanded during cold stages

The geographic origin of Pontic-Pannonian and south-western Siberian *A. austriacus* seems to be located in the eastern part of Europe in the Pontic (surroundings of the Black Sea) or Pannonian region, as suggested by the phylogenetic analysis of GBS data (Fig. 2). This is in line with traditional hypotheses of Meusel et al. (1965), who noted that the Pontic and Pannonian floristic regions are characterised by steppe plants that have a south-eastern European centre of development. However, a wider sampling would have allowed to pinpoint the primary source area of *A. austriacus* in this region more precisely; an origin in the

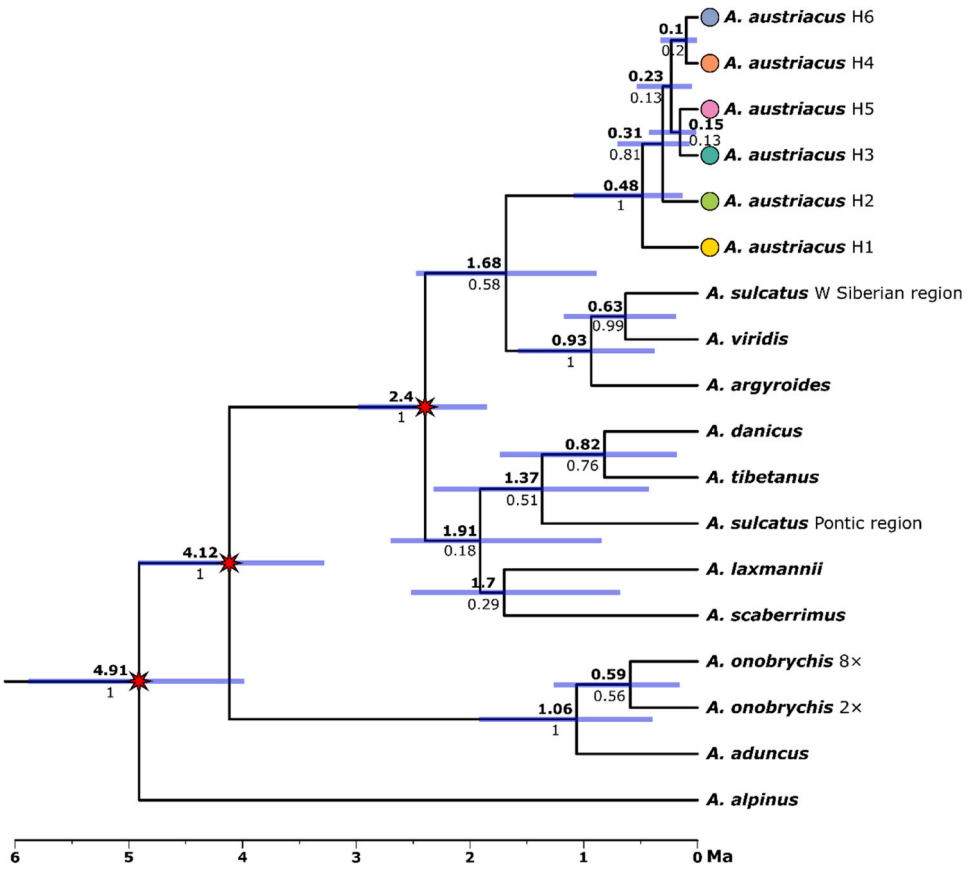

Fig. 5. Time-tree of the Hypoglottis clade of *Astragalus* (Azani et al., 2017, 2019) generated by Bayesian analysis of concatenated *mat*K and *ycf*1 sequences. Numbers above branches are the median heights (corresponding to age in millions of years) and numbers below branches are the posterior probabilities of nodes. The red stars indicate the calibration nodes after Su et al. (2021).

South Caucasus could as well be plausible given that this is the centre of diversification of many Eurasian *Astragalus* taxa (Maassoumi and Ashouri, 2022). Towards the east, populations of *A. austriacus* expanded their ranges across the Ural Mountains into the south-western Siberian region. Westwards the species colonised the Pannonian Basin. While we were able to outline a plausible evolutionary scenario for the populations of the main distribution area, the evolutionary links of these large populations to the few outpost populations of *A. austriacus* in the south-western Alps and north-eastern Iberia cannot be answered here and remain to be clarified. Given what is known from other steppe species, we speculate that these outposts might be old lineages rather than recent relics from a range expansion during the last glacial (Kirschner et al., 2020).

The distribution of haplotypes (*mat*K + *ycf*1) shows low geography-correlated differentiation most probably due to incomplete lineage sorting. The most common haplotype H2, which diversified further only in the Pontic area (H3–H6), was present in the entire Pannonian s.lat. and Pontic region. The higher haplotype diversity in the Pontic region (Pontic region: 4 haplotypes, Pannonian s.lat. region: 2 haplotypes) might indicate that colonisation of the Pannonian region happened from the Pontic area as suggested in the past (De Soó, 1929) and shown in other steppe species (Balashov et al., 2021; Seidl et al., 2021). A striking distribution pattern was found for the basalmost haplotype H1, which was detected in both the westernmost and easternmost parts of the sampled range, spanning over 4000 km (Fig. 4). Genetic connectivity across huge ranges was also observed in other steppe species, e.g., in *Cricetus cricetus* L. (Feoktistova et al., 2017). We interpret the occurrence of H1 at the edges of the sampled range as being relics of an initial expansion (ca. 240–480 ka; Figs. 5, 6). We want to point out that H1 might really be absent from the Pontic region, but we cannot exclude the possibility that we just missed to capture H1 in the Pontic region with our sampling. The presence of a unique ITS ribotype on the one hand in a population at the westernmost border of the sampled area (P2) and on the other hand in the two south-western Siberian populations could indicate an independent evolutionary history of these populations.

In addition to the main genetic split between the Pannonian s.lat. and Pontic/south-western Siberian populations (Fig. 2, 3), the LEA analysis of GBS data identified further substructure in the Pannonian s.lat. region, resulting in a total of three genetic groups and suggesting allopatric lineage formation in each of these areas: the Pannonian s.str. group located in the Pannonian Basin and surroundings, the Transylvanian group from the Transylvanian Basin, and finally a group distributed across the Pontic Plains to south-western Siberia. This reflects previous studies on steppe biota that have shown that areas such as the Pannonian Basin provided suitable long-term refugia for steppe elements also during warm and humid interglacials when forests expanded (Fekete et al., 2014; Kirschner et al., 2020; Magyari et al., 2010; Plenk et al., 2017, 2020; Říčanová et al., 2013; Willner et al., 2021; Záveská et al., 2019). Especially the topographically complex and hilly terrain along the margin of the Pannonian Basin (foothills of the Carpathians) might have offered suitable microclimates and ecotones for refugial survival in even the most unsuitable climatic conditions (Egorov et al., 2020; Magyari et al., 2014; Varga, 2010; Willner et al., 2021). The third genetic group includes all populations east of the Carpathians. Despite their large range, the populations of the Pontic and south-western Siberian region did not show a genetic substructure (Fig. 3 A). This suggests a recent and rapid colonisation of this huge area with recurrent gene flow. Further evidence for this scenario comes from the comparison of regional pAr which – due to the slow accumulation of new private alleles through mutation – is a good indicator for

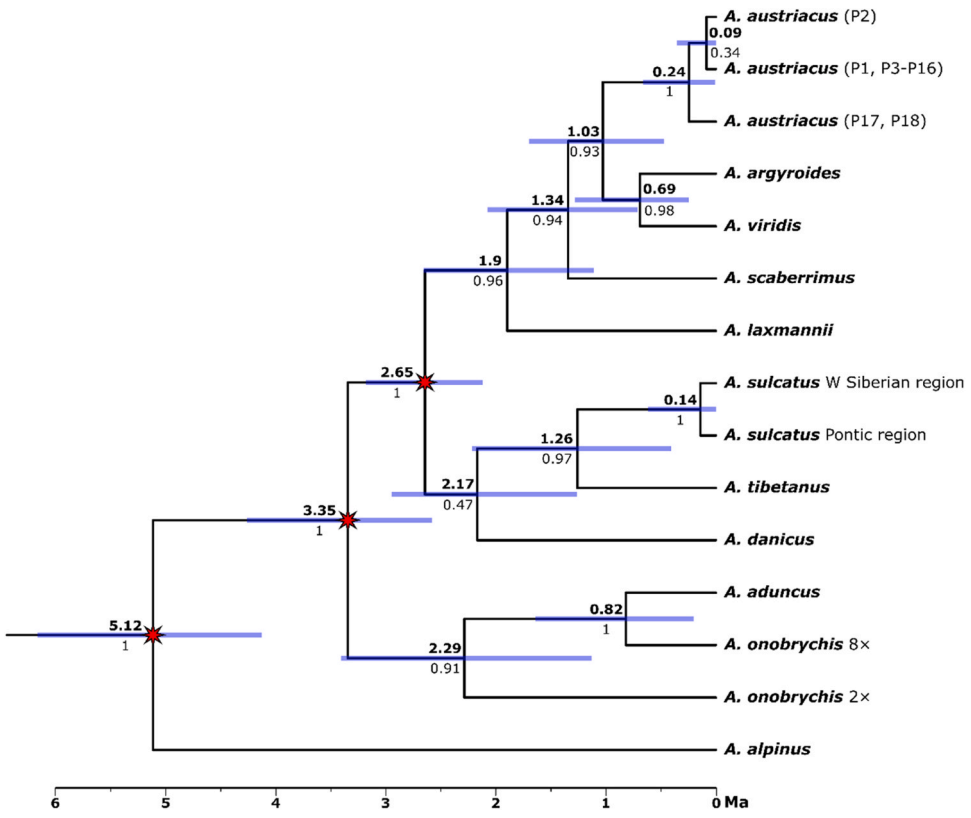

Fig. 6. Time-tree as in Fig. 5, calculated from ITS sequences. Numbers above branches are the median heights (corresponding to age in millions of years) and numbers below branches are the posterior probabilities of nodes. The red stars indicate the calibration nodes after Su et al. (2021).

long-lasting *in situ* persistence of populations. A slightly lower number of private alleles was found in the south-western Siberian region compared to the Pontic and Pannonian s.lat. region, while generally, the difference in the number of private alleles was small between areas, suggesting independent persistence in the three regions (Fig. S2).

Reconstruction of the demographic history of *A. austriacus* demonstrated that effective population sizes in the Pannonian s.lat. and Pontic regions were larger during the last cold stage and decreased postglacially (Fig. 3B). This hints to a dynamic scenario, in which populations and ranges of *A. austriacus* expanded during glacials and contracted during interglacials. At the same time this might have facilitated (recurrent) colonisation of new areas and secondary contact on the one hand, and extinction and/or the formation of allopatric lineages on the other hand. Such a dynamic has been demonstrated for Eurasian steppe biota using explicit demographic models (Campos et al., 2010; Garcia et al., 2011; Kirschner et al., 2023). Results from various case studies, which did not explicitly test such scenarios but utilised genetic information and/or niche models, came to similar conclusions. These studies focussed on a broad spectrum of steppe species, including plants (*Astragalus exscapus* L., Becker, 2013; *A. onobrychis*, Záveská et al., 2019; *Euphorbia seguieriana* Neck. s.lat., Frajman et al., 2019), beetles (*Hycleus polymorphus* Pallas, Riccieri et al., 2020), butterflies (*Pseudophilotes bavius* Eversmann, Sucháčková Bartoňová et al., 2020), and mammals (*Cricetus cricetus*, Feoktistova et al., 2017; *Lasiopodomys gregalis* Pallas, Baca et al., 2023; *Marmota* Blumenbach, Mills et al., 2023). Contrasting refugial dynamics, namely a lack of suitable LGM habitats in the Pontic steppes north and west of the Black Sea, have been suggested for some steppe plants including *A. austriacus* using ecological niche models backcasted to past climatic conditions (Divíšek et al., 2022). However, this would imply a large-scale population contraction of a steppe species in the last cold stage when steppe habitats were much larger than today and stands in contrast to the results of this study and genomic evidence from other Eurasian steppe biota (Kirschner et al., 2022).

4.3. Evolutionary commonalities and differences between *A. austriacus* and other typical steppe species

The phylogeography of *Adonis vernalis* was recently studied with GBS (Seidl et al., 2022) and revealed a similar pattern to *Astragalus austriacus*. In both cases the diversification and range expansion seemingly started in the region around the Black Sea, specifically in the eastern Pannonian region (*Ad. vernalis*) and in the wider Black Sea region (*A. austriacus*), respectively. Additionally, molecular dating revealed similar crown group ages and the initial lineage separation was found to have occurred in the Mid-Pleistocene after the MPT (*Ad. vernalis*: ~0.5 Ma, 95 % HPD ~1.5 Ma or younger; *A. austriacus*: ~0.48–0.24 Ma, 95 % HPD ~1.0 Ma or younger). A similar pattern with a possibly similar time of expansion was also found in the flightless steppe beetle *Lethrus apterus* (differentiation in a Pannonian and a Pontic lineage; Sramkó et al., 2022) and in the steppe ant *Plagiolepis taurica*, which differentiated in a "Balkanic-Pannonian" and a "Central Asian-Pontic" lineage probably after the MPT (Kirschner et al., 2023). The comparison of regional pAr, however, was somewhat different between *A. austriacus* and *Ad. vernalis*. The former species showed highly similar values for the Pontic and Pannonian s.lat. regions with a slight decrease towards the south-western Siberian region, whereas in *Ad. vernalis*, the highest value was found in the Pontic region and the lowest in the south-western Siberian region (Fig. S2; Seidl et al., 2022). The depletion of pAr in the Siberian region, which featured very dry, desert-like conditions during the last glacial (Sizikova and Zykina, 2015; Zykina and Zykin, 2003), is much more pronounced in *Ad. vernalis* than in *A. austriacus*. These results demonstrate that *A. austriacus* may have colonised Siberia east of the Ural Mountains earlier than *Ad. vernalis*, which could be related to differences in the ecological requirements of the two species.

Astragalus austriacus and *Ad. vernalis* (Seidl et al., 2022) are examples of steppe species with a comparably recent origin, given that they evolved after the MPT. In contrast, some Eurasian steppe biota,

including *Kraschenninnikovia ceratoides* (Seidl et al., 2020, 2021), *A. onobrychis* (Záveská et al., 2019), *Stipa breviflora* Griseb. (Ren et al., 2022), or steppe ants from the genus *Plagiolepis* (Kirschner et al., 2023) originated (significantly) earlier. Extant lineages of *K. ceratoides* diversified no later than around 2.2 ± 0.9 Ma, i.e., the initial divergence within the polyploid complex occurred in the earliest period of the Pleistocene (Gelasian) or even before (with a much older stem group) in western Central Asia and the Altai Region (Seidl et al., 2020, 2021). The initial divergence between the extant lineages of the *A. onobrychis* polyploid complex was estimated to be 2.3–1.0 Ma (Figs. 5, 6) in the Caucasus region with subsequent independent evolution of populations in the Balkans, the Pannonian and Pontic regions and the European Alps (Kirschner et al., 2020; Záveská et al., 2019). Diversification in a similar time horizon was suggested for *Plagiolepis* steppe ants, that speciated approximately 1.5–1.3 Ma as a consequence of warm stage steppe range contraction in western and central Europe (Kirschner et al., 2022, 2023). Because global cooling, aridification, and increased seasonality of the climate led to an opening of the landscape and the spread of modern types of steppes starting from continental Asia in the Pliocene/Lower Early Pleistocene (Gelasian, 2.6–1.8 Ma; Hurka et al., 2019; Pisareva et al., 2019; Willis and McElwain, 2002), Euro-Siberian steppe species likely formed anew in Asia during this time. Subsequent contractions of open grassland vegetation likely led to recurrent isolation of populations and facilitated lineage diversification (Baca et al., 2023; Kirschner et al., 2020, 2023). In the later phases of the Pleistocene, the areas of origin of the younger Euro-Siberian steppe species may have been anywhere between the Altai in the east and the Mediterranean in the west. Whether these diversification histories at different time horizons are stochastic events or are connected to the respective species ecological needs, remains to be clarified and could be a topic for future studies.

CRediT authorship contribution statement

Corinna Schmiderer: Writing – review & editing, Investigation. **Clemens Maylandt:** Writing – original draft, Visualization, Investigation, Formal analysis. **Karl-Georg Bernhardt:** Writing – review & editing, Supervision, Investigation, Funding acquisition, Conceptualization. **Anna Seidl:** Writing – original draft, Visualization, Investigation, Formal analysis, Data curation. **Petr A. Kosachev:** Writing – review & editing, Investigation. **Gergely Király:** Writing – review & editing, Investigation. **Barbara Neuffer:** Writing – review & editing, Investigation, Funding acquisition, Conceptualization. **Karin Tremetsberger:** Writing – original draft, Visualization, Supervision, Investigation, Formal analysis. **Philipp Kirschner:** Writing – original draft, Visualization, Formal analysis. **Simon Pfanzelt:** Writing – review & editing, Investigation, Formal analysis. **Nikolai Friesen:** Writing – review & editing, Investigation, Funding acquisition, Conceptualization. **Alexander V. Poluyanov:** Writing – review & editing, Investigation. **Frank R. Blattner:** Writing – review & editing, Methodology, Investigation, Funding acquisition, Conceptualization. **Herbert Hurka:** Writing – review & editing, Investigation, Funding acquisition, Conceptualization.

Declaration of Competing Interest

The authors declare that they have no known competing financial interests or personal relationships that could have appeared to influence the work reported in this paper.

Data availability

Newly generated raw sequence data have been deposited in the EMBL-EBI ENA and NCBI GenBank databases (see Appendices A, B for accession numbers).

Acknowledgements

This research was funded by the Austrian Science Fund (FWF) [grant I 3002-B25] and the German Research Foundation (DFG) [grants BL 462/18-1, FR 1431/8-1 and NE 314/15-1]. For open access purposes, the authors have applied a CC BY public copyright license to any author accepted manuscript version arising from this submission. We would also like to express our sincere thanks to all the people who helped with the field collections.

Appendix A. Populations of *Astragalus austriacus* Jacq. used in this study, arranged from west to east according to their biogeographic region. The Pannonian s.str. and the Transylvanian region together constitute the Pannonian s.lat. region. The vouchers are stored at the University of Natural Resources and Life Sciences, Vienna, Austria (WHB) or Senckenberg Research Institute and Natural History Museum, Frankfurt/Main, Germany (FR; transferred from Osnabrück University, OSBU). The EMBL-EBI ENA and NCBI GenBank (Benson et al., 2013) accession numbers of the sequence data are also provided

	Sample	GBS	ITS	*mat*K	*ycf*1
Pannonian s.str. region					
1	Austria, Lower Austria, Föhrenberge W of Mödling, 48.0806° N, 16.2774° E, coll. by K. Tremetsberger (May 27, 2015), WHB 65697	ERS10741170–ERS10741174 (P022; 5 individuals)	OQ106919	OQ830531	OQ830500
2	Austria, Lower Austria, Blauer Berg SE of Oberschoderlee, 48.6419° N, 16.3479° E, coll. by K.-G. Bernhardt et al. (May 23, 2017), WHB 68960	ERS10741177–ERS10741179 (P024; 3 individuals)	OQ106920	OQ830532	OQ830501
3	Hungary, Győr-Moson-Sopron County, Szent Antal-dűlő S of Fertőrákos, 47.7076° N, 16.6413° E, coll. by G. Király (June 1, 2017), WHB 72555	ERS10741180–ERS10741184 (P097; 5 individuals)	OQ106921	OQ830533	OQ830502
4	Hungary, Győr-Moson-Sopron County, NE of Albertkázmérpuszta, Várbalog, 47.8661° N, 17.0435° E, coll. by G. Király (June 10, 2017), WHB 72558	ERS10741185–ERS10741189 (P098; 5 individuals)	—	—	—
5	Hungary, Bács-Kiskun County, Fülöpháza, 46.8702° N, 19.4237° E, coll. by K.-G. Bernhardt et al. (June 2, 2018), WHB 72051	ERS10741192–ERS10741196 (P154; 5 individuals)	OQ106922	OQ830534	OQ830503
Transylvanian region					
6	Romania, Cluj County, NNW of Suatu, 46.7964° N, 23.9541° E, coll. by K.-G. Bernhardt et al. (May 29, 2015), WHB 64912	ERS10741162–ERS10741166, ERS10741191 (P019; 6 ind.)	OQ106923	OQ830535	OQ830504
7	Romania, Mureș County, NNE of Șăulia, 46.6531° N, 24.2198° E, coll. by K.-G. Bernhardt et al. (May 30, 2015), WHB 64910, 64911	ERS10741167–ERS10741169 (P020; 3 individuals)	OQ106924	OQ830536	OQ830505
8	Romania, Mureș County, W of Târgu Mureș, SSE of Pănet, 46.5390° N, 24.4753° E, coll. by K.-G. Bernhardt et al. (May 28, 2015), WHB 64908, 64909	ERS10741157–ERS10741161 (P018; 5 individuals)	OQ106925	OQ830537	OQ830506
Pontic region					
9	Russia, Kursk Oblast, Peresyp', 51.0914° N, 36.4800° E, coll. by A. Seidl et al. (June 14, 2018), WHB 73155	ERS10741209–ERS10741213 (P176; 5 individuals)	OQ106926	OQ830538	OQ830507

(*continued on next page*)

(*continued*)

Sample		GBS	ITS	*matK*	*ycf*1
10	Russia, Kursk Oblast, N of Khonok, 51.6032° N, 36.8687° E, coll. by A. Seidl et al. (June 10, 2018), WHB 73162	ERS10741199–ERS10741203 (P172; 5 individuals)	OQ106927	OQ830539	OQ830508
11	Russia, Kursk Oblast, Beketovo, 51.4572° N, 37.8885° E, coll. by A. Seidl et al. (June 16, 2018), WHB 7315	ERS10741217–ERS10741221 (P180; 5 individuals)	OQ106928	OQ830540	OQ830509
12	Russia, Belgorod Oblast, Bely Kolodez' E of Novy Oskol, 50.7592° N, 37.9450° E, coll. by A. Seidl et al. (June 15, 2018), WHB 73156	ERS10741214–ERS10741216 (P178; 3 individuals)	OQ106929	OQ830541	OQ830510
13	Russia, Voronezh Oblast, Krasnogorovka, 49.9271° N, 40.7726° E, coll. by A. Seidl et al. (June 12, 2018), WHB 73163	ERS10741204–ERS10741208 (P175; 5 individuals)	OQ106930	OQ830542	OQ830511
14	Russia, Rostov Oblast, Rostov, Botanical Garden steppe reserve, 47.2348° N, 39.6567° E, coll. by S. Pfanzelt et al. (June 14, 2018), WHB 74128—74131	ERS10741223–ERS10741225 (P226; 2 ind. plus 1 replicate)	OQ106931, OQ106932	OQ830543, OQ830544	OQ830512, OQ830513
15	Russia, Rostov Oblast, W of Proletarka, 47.8795° N, 40.2121° E, coll. by S. Pfanzelt et al. (June 15, 2018), WHB 74135	ERS10741226–ERS10741230 (P227; 5 individuals)	OQ106933, OQ106934	OQ830545, OQ830546	OQ830514, OQ830515
16	Russia, Volgograd Oblast, between Khar'kovka and Gmelinka, 50.3975° N, 46.8514° E, coll. by S. Pfanzelt (August 10, 2019), no voucher	ERS10741262–ERS10741263 (P335; 2 individuals)	OQ106935, OQ106936	OQ830547, OQ830548	OQ830516, OQ830517
South-western Siberian region (= Western Siberian Lowland)					
17	Kazakhstan, Akmola Region, between Ekibastuz and Ereymentau, 51.6871° N, 73.4376° E, coll. by S. Pfanzelt et al. (June 14, 2019), WHB 74881	ERS10741232 (P320; 1 individual)	OQ106937	OQ830549	OQ830518
18	Kazakhstan, Pavlodar Region, 75 km SW of Ekibastuz, 51.4639° N, 74.3186° E, coll. by B. Neuffer et al. (June 4, 2017), OSBU 25899	ERS10741190 (P107; 1 individual)	OQ106938	OQ830550	OQ830519

Appendix B. *Astragalus* outgroup samples used for the construction of the GBS tree and of the time-trees with *A. austriacus* along with their EMBL-EBI ENA and NCBI GenBank (Benson et al., 2013) accession numbers with the sectional classification according to Podlech and Zarre (2013). WHB, herbarium of the University of Natural Resources and Life Sciences, Vienna, Austria

Sample	GBS	ITS	*matK*	*ycf*1
Sect. *Craccina*: *A. sulcatus* L.				
Russia, Samara Oblast, S of Krasnoarmeyskoe, 52.6674° N, 50.0354° E, coll. by S. Pfanzelt (August 15, 2019), no voucher	ERS10741264–ERS10741268 (P336; 5 individuals)	OQ106939, OQ106940	OQ830551, OQ830552	OQ830520, OQ830521
Kazakhstan, Kostanay Region, S of Kalinovka, 53.5715° N, 62.4608° E, coll. by S. Pfanzelt et al. (June 17, 2019), WHB 74891	ERS10741233–ERS10741238 (P321; 5 ind. plus 1 replicate)	OQ106941	OQ830553	OQ830522
Russia, Kurgan Oblast, N of Makushino, 55.2683° N, 67.2877° E, coll. by S. Pfanzelt et al. (June 22, 2019), WHB 74887	ERS10741239–ERS10741243 (P325; 5 individuals)	—	—	—
Russia, Omsk Oblast, W of Mar'yanovka, 54.9690° N, 72.5628° E, coll. by S. Pfanzelt et al. (June 23, 2019), WHB 74894	ERS10741244–ERS10741248 (P326; 5 individuals)	OQ106942	OQ830554	OQ830523
Russia, Omsk Oblast, E of Kormilovka, 54.9896° N, 74.2275° E, coll. by S. Pfanzelt et al. (June 23, 2019), WHB 74895	ERS10741249–ERS10741250 (P327: 2 individuals)	—	—	—
Russia, Novosibirsk Oblast, S of Barabinsk, 55.2723° N, 78.2852° E, coll. by S. Pfanzelt et al. (June 24, 2019), WHB 74896	ERS10741251–ERS10741255 (P328; 5 individuals)	OQ106943	OQ830555	OQ830524
Russia, Novosibirsk Oblast, NE of Zhulanka, 54.3851° N, 80.6662° E, coll. by S. Pfanzelt et al. (June 25, 2019), WHB 74899	ERS10741256 (P330; 1 individual)	—	—	—
Russia, Altai Krai, Proslaukha, 53.3401° N, 80.9572° E, coll. by S. Pfanzelt et al. (June 26, 2019), WHB 74902	ERS10741257–ERS10741261 (P332; 5 individuals)	OQ106944	OQ830556	OQ830525
Sect. *Hypoglottidei*: *A. danicus* Retz.				
Russia, Kursk Oblast, Zapovedniy S of Kursk, 51.5696° N, 36.0890° E, coll. by A. Seidl et al. (June 8, 2018), WHB 73209	ERS10741222 (P182; 1 individual)	OQ106945	OQ830557	OQ830526
Sect. *Hypoglottidei*: *A. tibetanus* Benth. ex Bunge				
Kazakhstan, Almaty Region, Altyn-Emel National Park, N of Kalinino, 44.3378° N, 78.8398° E, coll. by K.-G. Bernhardt et al. (July 20, 2019), WHB 76476	ERS10741231 (P291; 1 individual)	OQ106946	OQ830558	OQ830527
Sect. *Onobrychoidei*: *A. onobrychis* L., octoploids (see Záveská et al., 2019)				
Austria, Lower Austria, Blauer Berg SE of Oberschoderlee, 48.6419° N, 16.3479° E, coll. by K.-G. Bernhardt et al. (May 23, 2017), no voucher	ERS10741175–ERS10741176 (P024; 2 individuals)	OQ106947	OQ830559	OQ830528
Hungary, Győr-Moson-Sopron County, Sínai-hegy N of Bőny, 47.6757° N, 17.8869° E, coll. by K. Tremetsberger et al. (May 31, 2018), WHB 81417	ERS10741198 (P158; 1 individual)	OQ106948	OQ830560	OQ830529
Hungary, Győr-Moson-Sopron County, Alsó-Jeges SE of Nagyszentjános, 47.6893° N, 17.8940° E, coll. by K. Tremetsberger et al. (May 31, 2018), WHB 81416	ERS10741197 (P157; 1 individual)	OQ106949	OQ830561	OQ830530

Appendix C. Details of the *Astragalus* sequences downloaded from NCBI GenBank (Benson et al., 2013) and used with the new sequences for the generation of the time-trees (Figs. 5, 6) with the sectional classification according to Podlech and Zarre (2013). For the diploid *A. onobrychis* population 276, the *ycf*1 sequence of Záveská et al. (2019) was supplemented with ITS and *mat*K sequences. The two sequenced individuals of this population had identical sequences in each marker; for sampling information of this population refer to Záveská et al. (2019)

Section	Species	GenBank accession number (country; reference)		
		ITS	*matK*	*ycf*1
Dissitiflori	*A. argyroides* Beck	JQ685667 (Türkiye) (Dizkirici et al., 2014)	KM387658 (Türkiye) (Dizkirici Tekpinar et al., 2016)	KM071773 (Azerbaijan) (Bartha, 2012)

(*continued on next page*)

(*continued*)

Section	Species	GenBank accession number (country; reference)		
		ITS	*matK*	*ycf*1
Dissitiflori	*A. viridis* Bunge	JQ685697 (Türkiye) (Dizkirici et al., 2014)	KM387668 (Türkiye) (Dizkirici Tekpinar et al., 2016)	KM071800 (Armenia) (Bartha, 2012)
Komaroviella	*A. alpinus* L.	KX954891 (China) (Azani et al., 2017)	KX955060 (China) (Azani et al., 2017)	JQ801551 (Austria) (Bartha et al., 2012)
Onobrychoidei	*A. aduncus* Willd.	KX954888 (Iran) (Azani et al., 2017)	KX955059 (Iran) (Azani et al., 2017)	MK354097 (Iran) (Záveská et al., 2019)
Onobrychoidei	*A. laxmannii* Jacq.	KX954974 (Mongolia) (Azani et al., 2017)	KX955135 (Mongolia) (Azani et al., 2017)	MT786136 (China) (Liu et al., 2020)
Onobrychoidei	*A. onobrychis* L., diploid population 276 of Záveská et al. (2019)	OQ818193 (Ukraine) (this study)	OQ830562 (Ukraine) (this study)	MK354095 (Ukraine) (Záveská et al., 2019)
Trachycercis	*A. scaberrimus* Bunge	KJ999345 (China) (Zheng et al., 2014)	MW654102 (China) (Guo et al., 2021)	MW654102 (China) (Guo et al., 2021)

Appendix D. Supporting information

Supplementary data associated with this article can be found in the online version at doi:10.1016/j.ppees.2024.125800.

References

Amini, E., Kazempour-Osaloo, S., Maassoumi, A.A., Zare-Maivan, H., 2019. Phylogeny, biogeography and divergence times of *Astragalus* section *Incani* DC. (Fabaceae) inferred from nrDNA ITS and plastid *rpl*32-*trnL*$_{(UAG)}$ sequences. Nord. J. Bot. 37, e02059 https://doi.org/10.1111/njb.02059.

Azani, N., Bruneau, A., Wojciechowski, M.F., Zarre, S., 2017. Molecular phylogenetics of annual *Astragalus* (Fabaceae) and its systematic implications. Bot. J. Linn. Soc. 184, 347–365. https://doi.org/10.1093/botlinnean/box032.

Azani, N., Bruneau, A., Wojciechowski, M.F., Zarre, S., 2019. Miocene climate change as a driving force for multiple origins of annual species in *Astragalus* (Fabaceae, Papilionoideae). Mol. Phylogenet. Evol. 137, 210–221. https://doi.org/10.1016/j.ympev.2019.05.008.

Baca, M., Popović, D., Agadzhanyan, A.K., Baca, K., Conard, N.J., Fewlass, H., Filek, T., Golubiński, M., Horáček, I., Knul, M.V., Krajcarz, M., Krokhaleva, M., Lebreton, L., Lemanik, A., Maul, L.C., Nagel, D., Noiret, P., Primault, J., Rekovets, L., Rhodes, S.E., Royer, A., Serdyuk, N.V., Soressi, M., Stewart, J.R., Strukova, T., Talamo, S., Wilczyński, J., Nadachowski, A., 2023. Ancient DNA of narrow-headed vole reveal common features of the Late Pleistocene population dynamics in cold-adapted small mammals. Proc. R. Soc. Lond. B 290, 20222238. https://doi.org/10.1098/rspb.2022.2238.

Bagheri, A., Maassoumi, A.A., Rahiminejad, M.R., Brassac, J., Blattner, F.R., 2017. Molecular phylogeny and divergence times of *Astragalus* section *Hymenostegis*: An analysis of a rapidly diversifying species group in Fabaceae. Sci. Rep. 7, 14033 https://doi.org/10.1038/s41598-017-14614-3.

Bagheri, A., Maassoumi, A.A., Brassac, J., Blattner, F.R., 2023. Dated phylogeny of *Astragalus* section *Stereothrix* (Fabaceae) and allied taxa in the Hypoglottis clade. Biology 12, 138. https://doi.org/10.3390/biology12010138.

Balashov, I.A., Neiber, M.T., Hausdorf, B., 2021. Phylogeny, species delimitation and population structure of the steppe-inhabiting land snail genus *Helicopsis* in Eastern Europe. Zool. J. Linn. Soc. 193, 1108–1125. https://doi.org/10.1093/zoolinnean/zlaa156.

Bartha, L., 2012. Molecular phylogenetic studies on the European species of the genus *Astragalus* L. section *Dissitiflori*. (PhD Thesis) Babeș-Bolyai University, Cluj-Napoca, Romania.

Bartha, L., Sramkó, G., Dragoș, N., 2012. New PCR primers for partial *ycf*1 amplification in *Astragalus* (Fabaceae): Promising source for genus-wide phylogenies. Stud. UBB Biol. 57, 33–45.

Bartha, L., Dragoș, N., Molnár, V., A, Sramkó, G., 2013. Molecular evidence for reticulate speciation in *Astragalus* (Fabaceae) as revealed by a case study from sect. *Dissitiflori*. Botany 91, 702–714. https://doi.org/10.1139/cjb-2013-0036.

Becker, T., 2013. Die Steppenreliktart *Astragalus exscapus* – eine Schlüsselart der Steppenreste Mitteleuropas? In: Baumbach, H., Pfützenreuter, S. (Eds.), Steppenlebensräume Europas – Gefährdung, Erhaltungsmaßnahmen und Schutz. Thüringer Ministerium für Landwirtschaft, Forsten. Umwelt und Naturschutz (TMLFUN), Erfurt, Germany, pp. 69–90.

Benson, D.A., Cavanaugh, M., Clark, K., Karsch-Mizrachi, I., Lipman, D.J., Ostell, J., Sayers, E.W., 2013. GenBank. Nucleic Acids Res 41, D36–D42. https://doi.org/10.1093/nar/gks1195.

Binney, H., Edwards, M., Macias-Fauria, M., Lozhkin, A., Anderson, P., Kaplan, J.O., Andreev, A., Bezrukova, E., Blyakharchuk, T., Jankovska, V., Khazina, I., Krivonogov, S., Kremenetski, K., Nield, J., Novenko, E., Ryabogina, N., Solovieva, N., Willis, K., Zernitskaya, V., 2017. Vegetation of Eurasia from the last glacial maximum to present: Key biogeographic patterns. Quat. Sci. Rev. 157, 80–97. https://doi.org/10.1016/j.quascirev.2016.11.022.

Borisova, A.G., Goncharov, N.F., Gorshkova, S.G., Popov, M.G., Vasil'chenko, I.T., 1946. English translation 1986. Flora of the U.S.S.R., vol. XII: Leguminosae: Astragalus. Izdatel'stvo Akademii Nauk SSSR. USSR, Moscow, Leningrad.

Bouckaert, R., Vaughan, T.G., Barido-Sottani, J., Duchêne, S., Fourment, M., Gavryushkina, A., Heled, J., Jones, G., Kühnert, D., De Maio, N., Matschiner, M., Mendes, F.K., Müller, N.F., Ogilvie, H.A., du Plessis, L., Popinga, A., Rambaut, A., Rasmussen, D., Siveroni, I., Suchard, M.A., Wu, C.-H., Xie, D., Zhang, C., Stadler, T., Drummond, A.J., 2019. BEAST 2.5: An advanced software platform for Bayesian evolutionary analysis. PLoS Comput. Biol. 15, e1006650 https://doi.org/10.1371/journal.pcbi.1006650.

Braun-Blanquet, J., 1961. Die inneralpine Trockenvegetation. Fischer, Stuttgart, Germany.

Braun-Blanquet, J., de Bolós, O., 1957. Les groupements végétaux du bassin moyen de l'Ebre et leur dynamisme. . Estac. Exp. Aula Dei 5, 1–266.

Bunge, A., 1868. Generis Astragali species Gerontogeae. Pars prior: Claves diagnosticae. Mémoires de L'Académie Impériale des Sciences de St.-Pétersbourg. VIIe Série 11, 1–140.

Campos, P.F., Kristensen, T., Orlando, L., Sher, A., Kholodova, M.V., Götherström, A., Hofreiter, M., Drucker, D.G., Kosintsev, P., Tikhonov, A., Baryshnikov, G.F., Willerslev, E., Gilbert, M.T.P., 2010. Ancient DNA sequences point to a large loss of mitochondrial genetic diversity in the saiga antelope (*Saiga tatarica*) since the Pleistocene. Mol. Ecol. 19, 4863–4875. https://doi.org/10.1111/j.1365-294X.2010.04826.x.

Chytrý, M., Horsák, M., Danihelka, J., Ermakov, N., German, D.A., Hájek, M., Hájková, P., Kočí, M., Kubešová, S., Lustyk, P., Nekola, J.C., Pavelková Řičánková, V., Preislerová, Z., Resl, P., Valachovič, M., 2019. A modern analogue of the Pleistocene steppe-tundra ecosystem in southern Siberia. Boreas 48, 36–56. https://doi.org/10.1111/bor.12338.

Clement, M., Posada, D., Crandall, K.A., 2000. TCS: A computer program to estimate gene genealogies. Mol. Ecol. 9, 1657–1659. https://doi.org/10.1046/j.1365-294x.2000.01020.x.

Compagnoni, A., Levin, S., Childs, D.Z., Harpole, S., Paniw, M., Römer, G., Burns, J.H., Che-Castaldo, J., Rüger, N., Kunstler, G., Bennett, J.M., Archer, C.R., Jones, O.R., Salguero-Gómez, R., Knight, T.M., 2021. Herbaceous perennial plants with short generation time have stronger responses to climate anomalies than those with longer generation time. Nat. Commun. 12, 1824. https://doi.org/10.1038/s41467-021-21977-9.

Corrêa dos Santos, R.A., Goldman, G.H., Riaño-Pachón, D.M., 2017. ploidyNGS: Visually exploring ploidy with Next Generation Sequencing data. Bioinformatics 33, 2575–2576. https://doi.org/10.1093/bioinformatics/btx204.

Danecek, P., Auton, A., Abecasis, G., Albers, C.A., Banks, E., DePristo, M.A., Handsaker, R.E., Lunter, G., Marth, G.T., Sherry, S.T., McVean, G., Durbin, R., 1000 Genomes Project Analysis Group, 2011. The variant call format and VCFtools. Bioinformatics 27, 2156–2158. https://doi.org/10.1093/bioinformatics/btr330.

De Soó, R., 1929. Die Vegetation und die Entstehung der Ungarischen Puszta. J. Ecol. 17, 329–350. https://doi.org/10.2307/2256046.

Divíšek, J., Večeřa, M., Welk, E., Danihelka, J., Chytrý, K., Douda, J., Chytrý, M., 2022. Origin of the central European steppe flora: Insights from palaeodistribution modelling and migration simulations. Ecography 2022, e06293. https://doi.org/10.1111/ecog.06293.

Dizkirici, A., Ekici, M., Kaya, Z., 2014. Comparative molecular phylogenetics of *Astragalus* L. sections from Turkey with New World *Astragalus* species using nrDNA ITS sequences. Plant Syst. Evol. 300, 163–175. https://doi.org/10.1007/s00606-013-0868-9.

Dizkirici Tekpinar, A., Karaman Erkul, S., Aytaç, Z., Kaya, Z., 2016. Phylogenetic relationships between *Oxytropis* DC. and *Astragalus* L. species native to an Old World diversity center inferred from nuclear ribosomal ITS and plastid *matK* gene sequences. Turk. J. Biol. 40, 250–263. https://doi.org/10.3906/biy-1502-5.

Drummond, A.J., Rambaut, A., 2007. BEAST: Bayesian evolutionary analysis by sampling trees. BMC Evol. Biol. 7, 214. https://doi.org/10.1186/1471-2148-7-214.
Drummond, A.J., Ho, S.Y.W., Phillips, M.J., Rambaut, A., 2006. Relaxed phylogenetics and dating with confidence. PLoS Biol. 4, e88 https://doi.org/10.1371/journal.pbio.0040088.
Dvořák, F., Dadáková, B., Grüll, F., 1977. Studies of the morphology of chromosomes of some selected species. Folia Geobot. Phytotax. 12, 343–375. https://doi.org/10.1007/BF02890649.
Eaton, D.A.R., Overcast, I., 2020. ipyrad: Interactive assembly and analysis of RADseq datasets. Bioinformatics 36, 2592–2594. https://doi.org/10.1093/bioinformatics/btz966.
Egorov, A.V., Zernov, A.S., Onipchenko, V.G., 2020. North-Western Caucasus. In: Noroozi, J. (Ed.), Plant biogeography and vegetation of high mountains of Central and South-West Asia. Springer, Cham, Switzerland, pp. 315–360. https://doi.org/10.1007/978-3-030-45212-4.
Erdős, L., Ambarlı, D., Anenkhonov, O.A., Bátori, Z., Cserhalmi, D., Kiss, M., Kröel-Dulay, G., Liu, H., Magnes, M., Molnár, Z., Naqinezhad, A., Semenishchenkov, Y.A., Tölgyesi, C., Török, P., 2018. The edge of two worlds: A new review and synthesis on Eurasian forest-steppes. Appl. Veg. Sci. 21, 345–362. https://doi.org/10.1111/avsc.12382.
Fekete, G., Molnár, Z., Magyari, E., Somodi, I., Varga, Z., 2014. A new framework for understanding Pannonian vegetation patterns: Regularities, deviations and uniqueness. Community Ecol. 15, 12–26. https://doi.org/10.1556/ComEc.15.2014.1.2.
Fekete, G., Király, G., Molnár, Z., 2016. Delineation of the Pannonian vegetation region. Community Ecol. 17, 114–124. https://doi.org/10.1556/168.2016.17.1.14.
Feoktistova, N.Y., Meschersky, I.G., Bogomolov, P.L., Sayan, A.S., Poplavskaya, N.S., Surov, A.V., 2017. Phylogeographic structure of the Common hamster (*Cricetus cricetus* L.): Late Pleistocene connections between Caucasus and Western European populations. PLoS One 12, e0187527. https://doi.org/10.1371/journal.pone.0187527.
Frajman, B., Záveská, E., Gamisch, A., Moser, T., The STEPPE Consortium, Schönswetter, P., 2019. Integrating phylogenomics, phylogenetics, morphometrics, relative genome size and ecological niche modelling disentangles the diversification of Eurasian *Euphorbia seguieriana* s. l. (Euphorbiaceae). Mol. Phylogenet. Evol. 134, 238–252. https://doi.org/10.1016/j.ympev.2018.10.046.
Frichot, E., François, O., 2015. LEA: An R package for landscape and ecological association studies. Method. Ecol. Evol. 6, 925–929. https://doi.org/10.1111/2041-210X.12382.
Friesen, N., Zerdoner Calasan, A., Neuffer, B., German, D.A., Markov, M., Hurka, H., 2020. Evolutionary history of the Eurasian steppe plant *Schivereckia podolica* (Brassicaceae) and its close relatives. Flora 268, 151602. https://doi.org/10.1016/j.flora.2020.151602.
Garcia, J.T., Mañosa, S., Morales, M.B., Ponjoan, A., García de la Morena, E.L., Bota, G., Bretagnolle, V., Dávila, J.A., 2011. Genetic consequences of interglacial isolation in a steppe bird. Mol. Phylogenet. Evol. 61, 671–676. https://doi.org/10.1016/j.ympev.2011.07.017.
Guo, Y., Yao, B., Yuan, M., Li, J., 2021. The complete chloroplast genome and phylogenetic analysis of *Astragalus scaberrimus* Bunge 1833. Mitochondrial DNA B Resour. 6, 3364–3366. https://doi.org/10.1080/23802359.2021.1997108.
Gutenkunst, R.N., Hernandez, R.D., Williamson, S.H., Bustamante, C.D., 2009. Inferring the joint demographic history of multiple populations from multidimensional SNP frequency data. PLoS Genet 5, e1000695. https://doi.org/10.1371/journal.pgen.1000695.
Hall, T.A., 1999. BioEdit: A user-friendly biological sequence alignment editor and analysis program for Windows 95/98/NT. Nucleic Acids Symp. Ser. 41, 95–98.
Hardion, L., Dumas, P.-J., Abdel-Samad, F., Bou Dagher Kharrat, M., Surina, B., Affre, L., Médail, F., Bacchetta, G., Baumel, A., 2016. Geographical isolation caused the diversification of the Mediterranean thorny cushion-like *Astragalus* L. sect. *Tragacantha* DC. (Fabaceae). Mol. Phylogenet. Evol. 97, 187–195. https://doi.org/10.1016/j.ympev.2016.01.006.
Hays, J.D., Imbrie, J., Shackleton, N.J., 1976. Variations in the earth's orbit: Pacemaker of the ice ages. Science 194, 1121–1132. https://doi.org/10.1126/science.194.4270.1121.
Hegi, G., Gams, H., Marzell, H., 1975. Illustrierte Flora von Mitteleuropa, IV. Band, 3. Teil: Dicotyledones, 2. Teil, Leguminosae – Tropaeolaceae. Parey, Berlin, Hamburg, Germany.
Herbert, T.D., 2023. The Mid-Pleistocene Climate Transition. Annu. Rev. Earth Planet. Sci. 51, 389–418. https://doi.org/10.1146/annurev-earth-032320-104209.
Hurka, H., Friesen, N., Bernhardt, K.-G., Neuffer, B., Smirnov, S.V., Shmakov, A.I., Blattner, F.R., 2019. The Eurasian steppe belt: Status quo, origin and evolutionary history. Turczaninowia 22, 5–71. https://doi.org/10.14258/turczaninowia.22.3.1.
Jäger, E.J., 1971. Die pflanzengeographische Stellung der Steppen der Iberischen Halbinsel. Flora 160, 217–256. https://doi.org/10.1016/S0367-2530(17)31669-9.
Kajtoch, Ł., Cieślak, E., Varga, Z., Paul, W., Mazur, M.A., Sramkó, G., Kubisz, D., 2016. Phylogeographic patterns of steppe species in Eastern Central Europe: A review and the implications for conservation. Biodivers. Conserv. 25, 2309–2339. https://doi.org/10.1007/s10531-016-1065-2.
Kalinowski, S.T., 2005. HP-RARE 1.0: A computer program for performing rarefaction on measures of allelic richness. Mol. Ecol. Notes 5, 187–189. https://doi.org/10.1111/j.1471-8286.2004.00845.x.
Kalyaanamoorthy, S., Minh, B.Q., Wong, T.K.F., von Haeseler, A., Jermiin, L.S., 2017. ModelFinder: Fast model selection for accurate phylogenetic estimates. Nat. Methods 14, 587–589. https://doi.org/10.1038/nmeth.4285.
Kaplan, Z., Danihelka, J., Štěpánková, J., Ekrt, L., Chrtek Jr., J., Zázvorka, J., Grulich, V., Řepka, R., Prančl, J., Ducháček, M., Kúr, P., Šumberová, K., Brůna, J., 2016. Distributions of vascular plants in the Czech Republic, part 2. Preslia 88, 229–322. https://doi.org/10.23855/preslia.2023.001.
Kazemi, M., Kazempour Osaloo, S., Maassoumi, A.A., Pouyani, E.R., 2009. Molecular phylogeny of selected Old World *Astragalus* (Fabaceae): Incongruence among chloroplast *trnL-F*, *ndhF* and nuclear ribosomal DNA ITS sequences. Nord. J. Bot. 27, 425–436. https://doi.org/10.1111/j.1756-1051.2009.00285.x.
Kirschner, P., Záveská, E., Gamisch, A., Hilpold, A., Trucchi, E., Paun, O., Sanmartín, I., Schlick-Steiner, B.C., Frajman, B., Arthofer, W., The STEPPE Consortium, Steiner, F. M., Schönswetter, P., 2020. Long-term isolation of European steppe outposts boosts the biome's conservation value. Nat. Commun. 11, 1968. https://doi.org/10.1038/s41467-020-15620-2.
Kirschner, P., Perez, M.F., Záveská, E., Sanmartín, I., Marquer, L., Schlick-Steiner, B.C., Alvarez, N., the STEPPE Consortium, Steiner, F.M., Schönswetter, P., 2022. Congruent evolutionary responses of European steppe biota to late Quaternary climate change. Nat. Commun. 13, 1921. https://doi.org/10.1038/s41467-022-29267-8.
Kirschner, P., Seifert, B., Kröll, J., the STEPPE Consortium, Schlick-Steiner, B.C., Steiner, F.M., 2023. Phylogenomic inference and demographic model selection suggest peripatric separation of the cryptic steppe ant species *Plagiolepis pyrenaica* stat. rev. Mol. Ecol. 32, 1149–1168. https://doi.org/10.1111/mec.16828.
Larsson, A., 2014. AliView: A fast and lightweight alignment viewer and editor for large datasets. Bioinformatics 30, 3276–3278. https://doi.org/10.1093/bioinformatics/btu531.
Lavin, M., Herendeen, P.S., Wojciechowski, M.F., 2005. Evolutionary rates analysis of Leguminosae implicates a rapid diversification of lineages during the Tertiary. Syst. Biol. 54, 575–594. https://doi.org/10.1080/10635150590947131.
Leigh, J.W., Bryant, D., 2015. POPART: Full-feature software for haplotype network construction. Methods Ecol. Evol. 6, 1110–1116. https://doi.org/10.1111/2041-210X.12410.
Liu, X., Fu, Y.-X., 2020. Stairway Plot 2: Demographic history inference with folded SNP frequency spectra. Genome Biol. 21, 280. https://doi.org/10.1186/s13059-020-02196-9.
Liu, Y., Chen, Y., Fu, X., 2020. The complete chloroplast genome sequence of medicinal plant: *Astragalus laxmannii* (Fabaceae). Mitochondrial DNA B Resour. 5, 3643–3644. https://doi.org/10.1080/23802359.2020.1829122.
Maassoumi, A.A., Ashouri, P., 2022. The hotspots and conservation gaps of the mega genus *Astragalus* (Fabaceae) in the Old-World. Biodivers. Conserv. 31, 2119–2139. https://doi.org/10.1007/s10531-022-02429-2.
Magnes, M., Willner, W., Janišová, M., Mayrhofer, H., Afif Khouri, E., Berg, C., Kuzemko, A., Kirschner, P., Guarino, R., Rötzer, H., Belonovskaya, E., Berastegi, A., Biurrun, I., Garcia-Mijangos, I., Mašić, E., Dengler, J., Dembicz, I., 2021. Xeric grasslands of the inner-alpine dry valleys of Austria – new insights into syntaxonomy, diversity and ecology. Veg. Classif. Surv. 2, 133–157. https://doi.org/10.3897/VCS/2021/68594.
Magyari, E.K., Chapman, J.C., Passmore, D.G., Allen, J.R.M., Huntley, J.P., Huntley, B., 2010. Holocene persistence of wooded steppe in the Great Hungarian Plain. J. Biogeogr. 37, 915–935. https://doi.org/10.1111/j.1365-2699.2009.02261.x.
Magyari, E.K., Kuneš, P., Jakab, G., Sümegi, P., Pelánková, B., Schäbitz, F., Braun, M., Chytrý, M., 2014. Late Pleniglacial vegetation in eastern-central Europe: Are there modern analogues in Siberia? Quat. Sci. Rev. 95, 60–79. https://doi.org/10.1016/j.quascirev.2014.04.020.
Meusel, H., Jäger, E., Weinert, E., 1965. Vergleichende Chorologie der zentraleuropäischen Flora. Fischer, Jena, Germany.
Mills, K.K., Everson, K.M., Hildebrandt, K.B.P., Brandler, O.V., Steppan, S.J., Olson, L.E., 2023. Ultraconserved elements improve resolution of marmot phylogeny and offer insights into biogeographic history. Mol. Phylogenet. Evol. 184, 107785 https://doi.org/10.1016/j.ympev.2023.107785.
Ossowski, S., Schneeberger, K., Lucas-Lledó, J.I., Warthmann, N., Clark, R.M., Shaw, R. G., Weigel, D., Lynch, M., 2010. The rate and molecular spectrum of spontaneous mutations in *Arabidopsis thaliana*. Science 327, 92–94. https://doi.org/10.1126/science.1180677.
Pignatti, S., 2017. Flora d'Italia. Edagricole, Bologna, Italy.
Pisareva, V.V., Faustova, M.A., Zyuganova, I.S., Karpukhina, N.V., Zakharov, A.L., Konstantinov, E.A., Semenov, V.V., Kurbanov, R.N., 2019. Changes in the landscape and climate of Eastern Europe in the Early Pleistocene. Stratigr. Geol. Correl. 27, 475–497. https://doi.org/10.1134/S086959381904004X.
Plenk, K., Bardy, K., Höhn, M., Thiv, M., Kropf, M., 2017. No obvious genetic erosion, but evident relict status at the westernmost range edge of the Pontic-Pannonian steppe plant *Linum flavum* L. (Linaceae) in Central Europe. Ecol. Evol. 7, 6527–6539. https://doi.org/10.1002/ece3.2990.
Plenk, K., Willner, W., Demina, O.N., Höhn, M., Kuzemko, A., Vassilev, K., Kropf, M., 2020. Phylogeographic evidence for long-term persistence of the Eurasian steppe plant *Astragalus onobrychis* in the Pannonian region (eastern Central Europe). Flora 264, 151555. https://doi.org/10.1016/j.flora.2020.151555.
Podlech, D., 1999. 27. Astragalus L. In: Talavera, S., Aedo, C., Castroviejo, S., Romero Zarco, C., Sáez, L., Salgueiro, F.J., Velayos, M. (Eds.), Flora iberica, vol. VII (I): Leguminosae (partim). Real Jardín Botánico. CSIC, Madrid, Spain, pp. 279–338.
Podlech, D., Zarre, S., 2013. A taxonomic revision of the genus *Astragalus* L. (Leguminosae) in the Old World, vol. I–III. Naturhistorisches Museum Wien, Vienna, Austria.
Polyakova, M.A., Dembicz, I., Becker, T., Becker, U., Demina, O.N., Ermakov, N., Filibeck, G., Guarino, R., Janišová, M., Jaunatre, R., Kozub, Ł., Steinbauer, M.J., Suzuki, K., Dengler, J., 2016. Scale- and taxon-dependent patterns of plant diversity in steppes of Khakassia, South Siberia (Russia). Biodivers. Conserv. 25, 2251–2273. https://doi.org/10.1007/s10531-016-1093-y.

Rambaut, A., Drummond, A.J., Xie, D., Baele, G., Suchard, M.A., 2018. Posterior summarization in Bayesian phylogenetics using Tracer 1.7. Syst. Biol. 67, 901–904. https://doi.org/10.1093/sysbio/syy032.

Ren, J., Yan, D., Ma, Y., Liu, J., Su, Z., Ding, Y., Wang, P., Dang, Z., Niu, J., 2022. Combining phylogeography and landscape genetics reveals genetic variation and distribution patterns of *Stipa breviflora* populations. Flora 293, 152102. https://doi.org/10.1016/j.flora.2022.152102.

Říčanová, Š., Koshev, Y., Říčan, O., Ćosić, N., Ćirović, D., Sedláček, F., Bryja, J., 2013. Multilocus phylogeography of the European ground squirrel: Cryptic interglacial refugia of continental climate in Europe. Mol. Ecol. 22, 4256–4269. https://doi.org/10.1111/mec.12382.

Riccieri, A., Mancini, E., Iannella, M., Salvi, D., Bologna, M.A., 2020. Phylogenetics and population structure of the steppe species *Hycleus polymorphus* (Coleoptera: Meloidae: Mylabrini) reveal multiple refugia in Mediterranean mountain ranges. Biol. J. Linn. Soc. 130, 507–519. https://doi.org/10.1093/biolinnean/blaa056.

Seidl, A., Pérez-Collazos, E., Tremetsberger, K., Carine, M., Catalán, P., Bernhardt, K.-G., 2020. Phylogeny and biogeography of the Pleistocene Holarctic steppe and semi-desert goosefoot plant *Krascheninnikovia ceratoides*. Flora 262, 151504. https://doi.org/10.1016/j.flora.2019.151504.

Seidl, A., Tremetsberger, K., Pfanzelt, S., Blattner, F.R., Neuffer, B., Friesen, N., Hurka, H., Shmakov, A., Batlai, O., Žerdoner Čalasan, A., Vesselova, P.V., Bernhardt, K.-G., 2021. The phylogeographic history of *Krascheninnikovia* reflects the development of dry steppes and semi-deserts in Eurasia. Sci. Rep. 11, 6645. https://doi.org/10.1038/s41598-021-85735-z.

Seidl, A., Tremetsberger, K., Pfanzelt, S., Lindhuber, L., Kropf, M., Neuffer, B., Blattner, F. R., Király, G., Smirnov, S.V., Friesen, N., Shmakov, A.I., Plenk, K., Batlai, O., Hurka, H., Bernhardt, K.-G., 2022. Genotyping-by-sequencing reveals range expansion of *Adonis vernalis* (Ranunculaceae) from Southeastern Europe into the zonal Euro-Siberian steppe. Sci. Rep. 12, 19074 https://doi.org/10.1038/s41598-022-23542-w.

Sizikova, A.O., Zykina, V.S., 2015. The dynamics of the Late Pleistocene loess formation, Lozhok section, Ob loess Plateau, SW Siberia. Quat. Int. 365, 4–14. https://doi.org/10.1016/j.quaint.2014.09.030.

Sramkó, G., Kosztolányi, A., Levente, L., Rácz, R., Szatmári, L., Varga, Z., Barta, Z., 2022. Range-wide phylogeography of the flightless steppe beetle *Lethrus apterus* (Geotrupidae) reveals recent arrival to the Pontic Steppes from the west. Sci. Rep. 12, 5069. https://doi.org/10.1038/s41598-022-09007-0.

Stamatakis, A., 2014. RAxML version 8: A tool for phylogenetic analysis and post-analysis of large phylogenies. Bioinformatics 30, 1312–1313. https://doi.org/10.1093/bioinformatics/btu033.

Stamatakis, A., Hoover, P., Rougemont, J., 2008. A rapid bootstrap algorithm for the RAxML Web servers. Syst. Biol. 57, 758–771. https://doi.org/10.1080/10635150802429642.

Stewart, J.R., Lister, A.M., Barnes, I., Dalén, L., 2010. Refugia revisited: Individualistic responses of species in space and time. Proc. Biol. Sci. 277, 661–671. https://doi.org/10.1098/rspb.2009.1272.

Su, C., Duan, L., Liu, P., Liu, J., Chang, Z., Wen, J., 2021. Chloroplast phylogenomics and character evolution of eastern Asian *Astragalus* (Leguminosae): Tackling the phylogenetic structure of the largest genus of flowering plants in Asia. Mol. Phylogenet. Evol. 156, 107025 https://doi.org/10.1016/j.ympev.2020.107025.

Sucháčková Bartoňová, A., Konvička, M., Marešová, J., Kolev, Z., Wahlberg, N., Fric, Z. F., 2020. Recently lost connectivity in the Western Palaearctic steppes: The case of a scarce specialist butterfly. Conserv. Genet. 21, 561–575. https://doi.org/10.1007/s10592-020-01271-9.

Sun, Y., Skinner, D.Z., Liang, G.H., Hulbert, S.H., 1994. Phylogenetic analysis of *Sorghum* and related taxa using internal transcribed spacers of nuclear ribosomal DNA. Theor. Appl. Genet. 89, 26–32. https://doi.org/10.1007/BF00226978.

Varga, Z., 2010. Extra-Mediterranean refugia, post-glacial vegetation history and area dynamics in Eastern Central Europe. In: Habel, J.C., Assmann, T. (Eds.), Relict species: Phylogeography and conservation biology. Springer, Berlin, Heidelberg, Germany, pp. 57–87. https://doi.org/10.1007/978-3-540-92160-8.

Vojtěchová, K., Kobrlová, L., Schönswetter, P., Duchoslav, M., 2023. Disentangling the taxonomic structure of the *Allium paniculatum* species complex in central and eastern Europe using molecular, cytogenetic and morphological tools. Preslia 95, 119–163. https://doi.org/10.23855/preslia.2023.119.

Weiß, C.L., Pais, M., Cano, L.M., Kamoun, S., Burbano, H.A., 2018. nQuire: A statistical framework for ploidy estimation using next generation sequencing. BMC Bioinforma. 19, 122. https://doi.org/10.1186/s12859-018-2128-z.

Wendler, N., Mascher, M., Nöh, C., Himmelbach, A., Scholz, U., Ruge-Wehling, B., Stein, N., 2014. Unlocking the secondary gene-pool of barley with next-generation sequencing. Plant Biotechnol. J. 12, 1122–1131. https://doi.org/10.1111/pbi.12219.

Wesche, K., Ambarlı, D., Kamp, J., Török, P., Treiber, J., Dengler, J., 2016. The Palaearctic steppe biome: A new synthesis. Biodivers. Conserv. 25, 2197–2231. https://doi.org/10.1007/s10531-016-1214-7.

White, T.J., Bruns, T., Lee, S., Taylor, J., 1990. Amplification and direct sequencing of fungal ribosomal RNA genes for phylogenetics. In: Innis, M.A., Gelfand, D.H., Sninsky, J.J., White, T.J. (Eds.), PCR protocols: A guide to methods and applications. Academic Press, San Diego, California, USA, pp. 315–322. https://doi.org/10.1016/B978-0-12-372180-8.50042-1.

Willis, K.J., McElwain, J.C., 2002. The Evolution of Plants. Oxford University Press, Oxford, UK.

Willner, W., Kuzemko, A., Dengler, J., Chytrý, M., Bauer, N., Becker, T., Biţă-Nicolae, C., Botta-Dukát, Z., Čarni, A., Csiky, J., Igić, R., Kącki, Z., Korotchenko, I., Kropf, M., Krstivojević-Ćuk, M., Krstonošić, D., Rédei, T., Ruprecht, E., Schratt-Ehrendorfer, L., Semenishchenkov, Y., Stančić, Z., Vashenyak, Y., Vynokurov, D., Janišová, M., 2017. A higher-level classification of the Pannonian and western Pontic steppe grasslands (Central and Eastern Europe). Appl. Veg. Sci. 20, 143–158. https://doi.org/10.1111/avsc.12265.

Willner, W., Moser, D., Plenk, K., Aćić, S., Demina, O.N., Höhn, M., Kuzemko, A., Roleček, J., Vassilev, K., Vynokurov, D., Kropf, M., 2021. Long-term continuity of steppe grasslands in eastern Central Europe: Evidence from species distribution patterns and chloroplast haplotypes. J. Biogeogr. 48, 3104–3117. https://doi.org/10.1111/jbi.14269.

Wilson, J.B., Peet, R.K., Dengler, J., Pärtel, M., 2012. Plant species richness: The world records. J. Veg. Sci. 23, 796–802. https://doi.org/10.1111/j.1654-1103.2012.01400.x.

Wojciechowski, M.F., 2005. *Astragalus* (Fabaceae): A molecular phylogenetic perspective. Brittonia 57, 382–396. https://doi.org/10.1663/0007-196X(2005)057[0382:AFAMPP]2.0.CO;2.

Wojciechowski, M.F., Lavin, M., Sanderson, M.J., 2004. A phylogeny of legumes (Leguminosae) based on analysis of the plastid *matK* gene resolves many well-supported subclades within the family. Am. J. Bot. 91, 1846–1862. https://doi.org/10.3732/ajb.91.11.1846.

Záveská, E., Maylandt, C., Paun, O., Bertel, C., Frajman, B., The STEPPE Consortium, Schönswetter, P., 2019. Multiple auto- and allopolyploidisations marked the Pleistocene history of the widespread Eurasian steppe plant *Astragalus onobrychis* (Fabaceae). Mol. Phylogenet. Evol. 139, 106572 https://doi.org/10.1016/j.ympev.2019.106572.

Žerdoner Čalasan, A., Hurka, H., German, D.A., Pfanzelt, S., Blattner, F.R., Seidl, A., Neuffer, B., 2021. Pleistocene dynamics of the Eurasian steppe as a driving force of evolution: Phylogenetic history of the genus *Capsella* (Brassicaceae). Ecol. Evol. 11, 12697–12713. https://doi.org/10.1002/ece3.8015.

Zheng, S., Liu, D., Ren, W., Fu, J., Huang, L., Chen, S., 2014. Integrated analysis for identifying Radix Astragali and its adulterants based on DNA barcoding. Evid. -Based Complement. Altern. Med. 2014, 843923 https://doi.org/10.1155/2014/843923.

Zykina, V.S., Zykin, V.S., 2003. Pleistocene warming stages in Southern West Siberia: Soils, environment, and climate evolution. Quat. Int. 106–107, 233–243. https://doi.org/10.1016/S1040-6182(02)00175-1.